NTNU – Trondheim
Norwegian University of
Science and Technology

Analysis of the Slow Floating in Grid Frequency of the Nordic Power System

Impact of Hydraulic System Characteristics

Magnus Grøtterud

Master of Energy and Environmental Engineering
Submission date: June 2012
Supervisor: Kjetil Uhlen, ELKRAFT
Co-supervisor: Trond Toftevaag, SINTEF Energy Research

Norwegian University of Science and Technology
Department of Electric Power Engineering

Problem description

In the Nordic synchronous system a slow floating in grid frequency (11-17 mHz) has been observed. The reason for this floating in grid frequency is not known, but it is assumed that it will cause increased wear of the turbines that are supplying primary control. Vattenfall AB has investigated how turbine governor parameters affect this phenomenon.

In this Master's Thesis work the following questions should be considered: Can choice of parameters for the turbine governor cause low-frequency oscillations in the Nordic synchronous system? Are these oscillations caused by the present hydro turbine governor tuning? How can these oscillations be avoided? Is the reason for the oscillations connected to other dynamics, for example hydraulic system conditions, voltage control, power system stabilizers?

The work will comprise modelling and simulation of an equivalent of the Nordic power system. The modelling should take adequate account of the hydraulic system and the restrictions related to this.

Abstract

This Master's Thesis work deals with the analysis of the observed slow floating in the grid frequency of the Nordic power system. Measurements indicate that the frequency of this floating or oscillation is around 11-17 mHz. The reason for this floating is not known to this date, but it is suspected that it will increase the wear of the turbines that are providing primary regulation.

In this work possible interaction between the hydraulic system and the power system has been emphasized and whether the governor settings may influence the slow floating, or not. The hydraulic models for the water conduit and turbine that are implemented in power system analysis tools are often simplified. In this Master's Thesis a hydraulic model that includes the effect of water hammer, surge tank and head loss has been implemented in the analysis tool SIMPOW®. A three-machine equivalent of the Norwegian and Swedish power system has been established to study the response of the frequency after a severe disturbance.

It has been demonstrated that for a severe disturbance a low-frequency mass oscillation will occur in the tunnel between the surge tank and the reservoir in the model. This will cause an oscillation in the pressure at the turbine which affects the grid frequency. The frequency of the mass oscillation depends on the construction of the tunnel and surge tank and will be different for every hydro power plant. Frequencies in the range of 5-11 mHz was found for the model used in this Thesis. It has been illustrated that with different characteristics for the two hydro power plants in the model, the floating in power system frequency will be the sum of the mass oscillations, which is assumed to be the case for the real power system. The governor parameters are found to have little influence on the damping of the low-frequency oscillations.

For further work a study of the impact of several different hydro power plants in a more extensive equivalent of the Nordic power system is suggested. For this work emphasis should be on finding parameters for typical Norwegian and Swedish hydro power plants.

Sammendrag

Denne masteroppgaven tar for seg en analyse av en observert langsom pendling på 11-17 mHz i frekvensen i det nordiske kraftsystemet. Grunnen til denne pendlingen er ikke kjent til dags dato, men det mistenkes at den vil øke slitasjen av turbiner som bidrar til primær regulering.

I dette arbeidet er det lagt hovedvekt på å analysere en mulig interaksjon mellom det hydrauliske systemet og kraftsystemet og om turbinregulatorens innstillinger kan ha innflytelse på den langsomme pendlingen. De hydrauliske modellene for vannvei og turbin som er implementert i kraftsystemsimuleringsverktøy er ofte forenklet. I denne masteroppgaven er en hydraulisk modell som ivaretar effekten av trykkstøt, svingekammer og trykktap blitt implementert i simuleringsverktøyet SIMPOW®. En stilisert tre-maskin ekvivalent for det norske og svenske kraftsystemet er etablert for å studere forløpet til frekvensen etter en større forstyrrelse.

Det er vist at for en alvorlig forstyrrelse vil det oppstå en lavfrekvent masse-svingning i tunnelen mellom svingekammeret og reservoaret i modellen. Dette forårsaker svingning i trykket ved turbinen som påvirker frelvensen i nettet. Frekvensen til massesvingningen er avhengig av tunnelens og svingekammerets konstruksjon og vil være forskjellig for alle vannkraftverk. For modellen brukt i denne oppgaven ble det påvist svingninger med frekvens i området 5-11 mHz. Det er vist at når de to vannkraftverkene i modellen har ulike hydrauliske karakteristika vil pendlingen i frekvensen være en sum av massesvingningene, noe som antas å være tilfelle i det virkelige kraftsystemet. Turbinregulatorens parametere er funnet å ha liten innflytelse på demping av de lavfrekvente svingningene i frekvensen.

For videre arbeid er en studie av virkningen av flere forskjellige vannkraftverk i en mer omfattende ekvivalent for det nordiske kraftsystemet foreslått. I et slikt arbeid bør det legges vekt på å finne parametere for typiske norske og svenske vannkraftverk.

Preface

This is my Master's Thesis in Electrical Power Engineering. It was carried out at the Faculty of Information Technology, Mathematics and Electrical Engineering at the Norwegian University of Science and Technology spring 2012.

I would like to thank Kjetil Uhlen who has been my supervisor and has given me constructive advice all the way along. A special thanks to my co-supervisor Trond Toftevaag who always were there to listen and help me think through my problems. He has also been very enthusiastic about this Master's Thesis which has been inspirational. I would also like to thank Bjørnar Svingen at Rainpower who has helped me better understand the hydraulic system at hydro power stations.

Magnus Grøtterud
Trondheim, Norway
June 2012

Contents

List of Figures

List of Tables

Symbols and Abbreviations

Notation

Italic font denotes standard variables and coefficients

Bold font denotes matrices

Symbols

$\lambda = \sigma \pm j\omega$	Eigenvalue with real and complex part
$\mathbf{A}$	System state matrix
$\mathbf{I}$	Diagonal identity matrix
ω_m	Mass oscillation frequency [rad/s]
A_p	Penstock cross section [m^2]
A_s	Surge tank cross section [m^2]
A_T	Proportional factor. Transform pu torque of turbine to pu torque of generator
C_s	Surge tank storage constant [s]
D	Turbine damping
d	Diameter of tunnel, penstock or surge tank [m]
E''_d	d-axis component of the subtransient internal emf
E''_q	q-axis component of the subtransient internal emf
E'_d	d-axis component of the transient internal emf
E'_q	q-axis component of the transient internal emf
f_0	Surge tank head loss coefficient [$m/(m^3/s)^2$]
f_{p1}	Penstock head loss coefficient [$m/(m^3/s)^2$]
f_{p2}	Tunnel head loss coefficient [$m/(m^3/s)^2$]
G	Gate opening
g	Acceleration of gravity 9.81 [m/s^2]
h	Head [m]
h_l	Head loss [m]
h_r	Head at rated flow [pu]
h_{base}	Rated turbine head [m]
J	Inertia [s]

L	Length of tunnel, penstock or surge tank [m]
L_p	Penstock length [m]
M	Coefficient of inertia
P_{el}	Electrical power demand in the network [W]
P_{mec}	Mechanical power developed in the turbine [W]
q	Flow [m^3/s]
q_r	Flow at rated load [pu]
q_{base}	Rated flow [m^3/s]
q_{nl}	No-load flow [m^3/s]
R_P	Permanent droop
R_T	Transient or temporary droop
s	The Laplace operator
T'_{d0}, T''_{d0}	d-axis open-circuit transient and subtransient time constant [s]
T'_{q0}, T''_{q0}	q-axis open-circuit transient and subtransient time constant [s]
T_e	Water starting time [s]
T_M	Mechanical time constant
T_w	Water starting time [s]
T_{el}	Electrical torque on the shaft. Produced in the generator [Nm]
T_{mec}	Mechanical torque on the shaft. Produced in the turbine [Nm]
v	Wave travel time [m/s]
X_d, X'_d, X''_d	d-axis synchronous, transient and subtransient reactance
X_q, X'_q, X''_q	q-axis synchronous, transient and subtransient reactance
Z_0	Surge impedance for conduit

Abbreviations

AB	Aksje Bolag. Limited company (stock corporation)
d-axis	Direct axis of a generator
DSL	Dynamic Simulation Language
emf	Electro-motive force
IEEE	Institute of Electrical and Electronics Engineers
NTH	Norwegian Institute of Technology - forerunner of NTNU
NTNU	Norwegian University of Science and Technology
PID	Proportional-integral-derivative controller
PSS	Power System Stabilizer
PSS®E	Power System Simulator for Engineering tool developed by SIEMENS
pu	Per unit
q-axis	Quadrature axis of a generator
TSO	Transmission System Operator. In Norway the TSO is Statnett

Chapter 1

Introduction

1.1 Background

In 2010 a project was initiated by the Swedish company Vattenfall Vattenkraft AB in order to investigate the slow floating in the grid frequency of the Nordic power system. It is not known what is feeding this variation in frequency but it is suspected that it will increase the wear of the generators that are providing primary regulation [1]. In research done by Vattenfall Research and Development AB the frequency variations were studied with the notion that it was caused by miss tuned settings for the turbine governor systems.

After the project was started in 2010 a work group for the study of this phenomenon has been established, *Measures to mitigate the frequency oscillations with a period of 60-90 seconds in the Nordic synchronous system.* This work group includes representatives from the different TSO's in the Nordic power system and expertise from research companies in Scandinavia.

The Swedish consulting company Gothia Power is one the of the work group members and has studied the frequency variations in order to find out at what frequencies the oscillations occur. By using different methods of spectral analysis the time period of 60-90 seconds, equivalent to frequencies of 11-17 mHz, has been found to be the most dominating [2]. This is presented in Figure 1.1 where the plot on top shows the measured frequency deviation in the Nordic power system and the plot underneath is the result of the different spectral analysis.

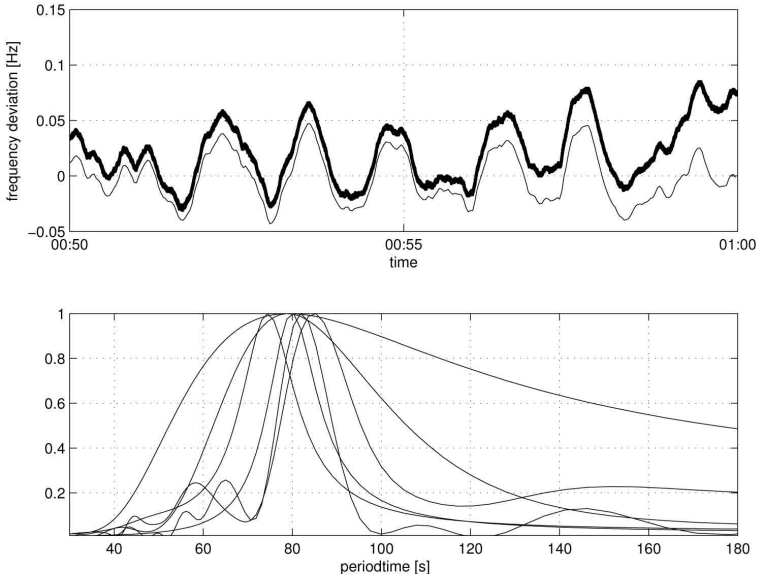

Figure 1.1 – Top, frequency deviation measured in the Nordic power system. Bottom, result of different methods of spectral analysis indicating that the oscillations occur with a period time of 60-90 seconds [2]

1.2 Objective

The purpose of this Master's Thesis is to find out if choice of parameters for the turbine governor system can contribute to the slow floating in frequency observed in the Nordic power system. This will be done by modelling and simulating an equivalent of the Norwegian and Swedish power system. The model should take adequate account of the hydraulic system and the restrictions related to this to make sure that possible interaction between the hydraulic system and the power system is included.

1.3 Scope of Work

Two detailed models for the hydraulic system will be presented and compared against a typical model implemented in power system analysis tools. The reason for this is to see if there are any hydraulic dynamics that are omitted in the models that are being used in standard power system stability studies. In this Thesis the

objective is to find out if the turbine governor system will have an impact on the floating in frequency, hence two hydro turbine governors will be presented.

A three machine equivalent of the Norwegian and Swedish power system is established and modelled in the simulation tool SIMPOW®. This Thesis will contain a case study where the response to a severe disturbance is simulated and the effect of governor parameters and different hydraulic systems are presented.

1.4 Outline of the Thesis

Chapter 2 are meant to give a short presentation of the Nordic power system and the power system stability topic. The method of eigenvalue analysis will also be described. Chapter 3 deals with the simulation tools used for analysis in this Thesis.

Chapter 4 starts with a description of hydro power plants. For the turbine and the water conduit equations are presented to be able to establish models used in simulations. Three different models for the hydraulic system are proposed and compared by frequency response. Chapter 5 presents the concept of the turbine governing system and why there is a need for it. Two different models for the hydro turbine governor are illustrated and compared.

Chapter 6 presents an equivalent of the Norwegian and Swedish power system and how the different dynamics are modelled in the case study of Chapter 7. In the case study the impact of detailed models for the hydraulic system and governor are studied in dynamic simulations.

In Chapter 8 the limitations in this Thesis are pointed out and the results are discussed. Chapter 9 presents the most important results and general conclusions are drawn. Finally, Chapter 10 suggest a scope for further work.

Chapter 2

Power Systems

This chapter will give a brief description of the Nordic power system and present the power system stability topic.

2.1 The Nordic Power System

The Nordic synchronous power system, or the Nordel system, comprises the power systems of the four countries Norway, Sweden, Finland and East-Denmark [3]. The national power systems are interconnected and has a common frequency of 50 Hz, which means they have to be controlled together as a synchronous system. Production systems differ greatly between the different countries. In Norway there is almost only hydro power while there in Denmark is a wide use of conventional thermal power plants and an increasing proportion of wind. Finland and Sweden has both a mix of different sources, but mostly hydro and nuclear (thermal) power.

2.2 Power System Stability

Power system stability is a large topic and is important for secure power system operation. This section will present different stability categories and important factors for stable operation.

2.2.1 Definitions

There are different definitions for power system stability, but the one that will be used here is the one defined by IEEE and CIGRE. "Power system stability is the

ability of an electric power system, for a given initial operating condition, to regain a state of operating equilibrium after being subjected to a physical disturbance, with most system variables bounded so that practically the entire system remains intact" [4]. Different sub-categories of stability will now be presented.

Rotor Angle Stability

Rotor angle stability refers to the ability of the synchronous machines of the power system to remain in synchronism after a disturbance has occurred[4]. This relates to the ability of the synchronous machines to maintain equilibrium between the mechanical torque and the electromagnetic torque. If rotor angle instability occurs the angular swings of the machine increase and the machine may loose synchronism with the rest of the generators in the grid.

Frequency Stability

Power system frequency is an important parameter in power system operation. To ensure safe operation of loads and generators a steady frequency is required. The frequency deviation, the difference between the reference frequency and the actual system frequency, must be controlled within certain limits. In the Nordic power system this is, 50 ± 0.1 Hz, and the frequency have to stay within these limits during normal disturbances. Frequency stability is defined as the systems ability to maintain steady frequency following a severe disturbance where there is a considerably large imbalance between load and generation [5, 4].

Voltage Stability

Voltage stability refers to the ability of the power system to maintain steady state voltages at all buses in the system after a disturbance [4]. If the voltage start to oscillate uncontrollably it can cause damage to equipment and tripping of lines which can give loss of loads and blackouts.

2.2.2 Power System Oscillations

The power systems are very complex and the electric power is highly alternating [6]. Three types of stability has been described in this chapter and all of them relates

to different oscillations that may occur due to disturbances. In [6] two main types of oscillations are presented; local and inter-area. The local modes of oscillations are connected to how one single generator will act against the total system and these modes have a natural frequency of 1 to 2 Hz. Inter-area modes are more complex and have frequencies of 0.1 to 0.7 Hz. These oscillations occur between big interconnected power systems and involves many generators. If all the generators in Norway swing against the generators in Sweden this is an inter-area mode. If the oscillation occur at even lower frequencies it can be called a global mode since all the units will swing together.

2.3 Eigenvalue Analysis

The method of eigenvalue analysis is presented in "Power System Dynamics" [7]. The main reason for using eigenvalue analysis is to simplify large dynamic systems by representing the system response as a linear combination of different responses, also called modes. A linear system can be represented as

$$\dot{\mathbf{x}} = \mathbf{A}\mathbf{x} \tag{2.1}$$

where $\mathbf{x}$ is the state vector and $\mathbf{A}$ is the $n \times n$ system state matrix.

2.3.1 Eigenvectors

The number λ represents an eigenvalue of a matrix $\mathbf{A}$ if there exists a non-zero column vector $\boldsymbol{\phi}$ that satisfy [8]:

$$\mathbf{A}\boldsymbol{\phi} = \lambda\boldsymbol{\phi} \tag{2.2}$$

The vector $\boldsymbol{\phi}$ is referred to as the right eigenvector associated with the eigenvalue λ. Equation 2.2 will have a non-trivial solution $\boldsymbol{\phi} \neq 0$ if

$$\det(\mathbf{A} - \lambda\mathbf{I}) = 0 \tag{2.3}$$

where $\mathbf{I}$ is the diagonal identity matrix. Equation 2.3 is also known as the characteristic equation. Similarly as for Equation 2.2 this can be written

$$\boldsymbol{\psi}\mathbf{A} = \lambda\boldsymbol{\psi} \tag{2.4}$$

where $\boldsymbol{\psi}$ is the left eigenvector. The left and right eigenvectors are orthogonal for different eigenvalues, so that if $\lambda_i \neq \lambda_j$,

$$\boldsymbol{\psi}_j \boldsymbol{\phi}_i = 0 \tag{2.5}$$

For eigenvectors corresponding to the same eigenvalue the eigenvectors are usually normalised so that

$$\boldsymbol{\psi}_i \boldsymbol{\phi}_i = 1 \tag{2.6}$$

2.3.2 Eigenvalues and Damping

The eigenvalues, λ_i, for the system can be found by solving Equation 2.3. The eigenvalues can either be real

$$\lambda_i = \sigma_i \tag{2.7}$$

or complex (as complex conjugated pairs)

$$\lambda_i = \sigma_i \pm j\omega_i \tag{2.8}$$

In "Power System Dynamics" the following conclusions are found to be important for analysing power system dynamics [7]:

1. Real eigenvalues introduce aperiodic modes that are proportional to $e^{\sigma_i t}$. If $\sigma_i < 0$ the aperiodic mode is stable. The mode is unstable for $\sigma_i > 0$.
2. Each conjugate pair of complex eigenvalues introduce oscillatory modes proportional to $e^{\sigma_i t}\cos(\omega_i t + \phi_{ki})$
3. A dynamic system described by Equation 2.1 is unstable if one of the modes are unstable.

The damping ratio is defined as

$$\zeta = \frac{-\sigma}{\sqrt{\sigma^2 + \omega^2}} \tag{2.9}$$

and [7] claims that the damping is satisfactory if the damping ratio $\zeta \geq 0.05$, but this depends on the variable that oscillates. The damping ratio can also be found by measuring the amplitude of the response. If x_1 is the value of one peak, relative

to the steady state value, and x_2 is the next peak, it is shown that [9]:

$$\zeta = \frac{\ln\left(\frac{x_1}{x_2}\right)}{\sqrt{\ln\left(\frac{x_1}{x_2}\right)^2 + (2\pi)^2}} \tag{2.10}$$

The damping ratio determines the rate of which the amplitude of the oscillation decays. There is two ways to increase the damping ratio:

1. Move the eigenvalue to the left in the complex plane. This means that σ will be more negative.
2. Move the eigenvalue towards the real axis by decreasing ω.

2.3.3 Sensitivity Analysis

Sensitivity of eigenvalues can give information on how the eigenvalue will change with a change of the elements in the state matrix, $\mathbf{A}$. If one differentiate Equation 2.2 with respect to a_{kj} (which is a element in the state matrix, kth row and jth column) one get [8]:

$$\frac{\partial \mathbf{A}}{\partial a_{kj}}\boldsymbol{\phi}_i + \mathbf{A}\frac{\partial \boldsymbol{\phi}_i}{\partial a_{kj}} = \frac{\partial \lambda_i}{\partial a_{kj}}\boldsymbol{\phi}_i + \lambda_i\frac{\partial \boldsymbol{\phi}_i}{\partial a_{kj}} \tag{2.11}$$

By pre multiplying with $\boldsymbol{\psi}_i$ this simplifies to:

$$\boldsymbol{\psi}_i\frac{\partial \mathbf{A}}{\partial a_{kj}}\boldsymbol{\phi}_i = \frac{\partial \lambda_i}{\partial a_{kj}} \tag{2.12}$$

In the matrix $\partial\mathbf{A}/\partial a_{kj}$ all elements are zero except for the ones in row kth row and jth colum which are 1. This means that Equation 2.12 simplifies to:

$$\frac{\partial \lambda_i}{\partial a_{kj}} = \boldsymbol{\psi}_{ik}\boldsymbol{\phi}_{ji} \tag{2.13}$$

Chapter 3

Simulation Software

3.1 SIMPOW®

SIMPOW® is a simulation tool made by the Swedish company STRI AB [10]. The software has modules for different types of power system analysis. Optpow is the module used to find the optimal power flow for a specific power system topology. The input for Optpow is given in a text file where busbars, lines, transformers, power productions and loads are defined. The result of the optimal power flow in Optpow gives an initial condition for the dynamic module, Dynpow.

Dynamical behaviour is added to the system in Dynpow. As for Optpow, the input for Dynpow is written in a text file. The power inputs can be set to be synchronous generators of various degree of detail with different kinds of turbines and regulation. The loads can be set to be dependent of frequency and voltage. Dynpow has a module for doing linear analysis where the eigenvalues for the system can be computed and different kinds of sensitivity analysis can be performed. It is also possible to do time domain analysis where you can define various faults and disconnections. This is of interest if one wants to find out if the system will regain a new steady state operating point after a fault.

DSL Code Generator is a tool used to build control system or other kind of dynamic systems. For cooperation with SIMPOW® there has been made a toolbox, designated to the different signals found in the dynamic system of Dynpow, for example frequency, gate position and mechanical torque. In the DSL Code Generator large systems can be built with standard included building blocks, like integrators, derivatives, filters and limiters. The result is compiled to a DSL-file which in turn can be implemented in Dynpow.

Chapter 4

Hydro Power Plants

This chapter will briefly explain the different parts of typical hydro power plants and how their hydraulics are modelled. The transformation of kinetic energy of water into mechanical energy of the prime mover is a complex process. It is necessary to have an understanding of how the water conduit and the turbines work and how their responses are like since it is of great importance for the turbine governor settings and for making detailed models for power system dynamic studies.

4.1 Introduction

One typical hydro power plant is illustrated in Figure 4.1. The water conduit consists of a reservoir, a low pressure tunnel, a surge tank and a high pressure penstock. The gate, which is located at the turbine, is controlled by the turbine governor and regulates the water flow. The turbine is connected to the prime mover and produces a mechanical torque which is used to generate voltage in a synchronous generator.

Figure 4.2 shows the relationship between the different dynamics of a hydro power plant. The turbine and conduit dynamics relates to the hydraulic part of the power plant that has to do with the energy conversion. Several models exist in literature and three of them will be studied in this chapter [12]. Chapter 5 will take care of the turbine control dynamics, which in this Thesis is referred to as the turbine governor dynamics. In this Thesis the main focus will be to study the turbine governor dynamics and modelling of the hydraulic dynamics, the automatic generation control will not be considered. The load and rotor dynamics are included in the models, but will not be explained in detail.

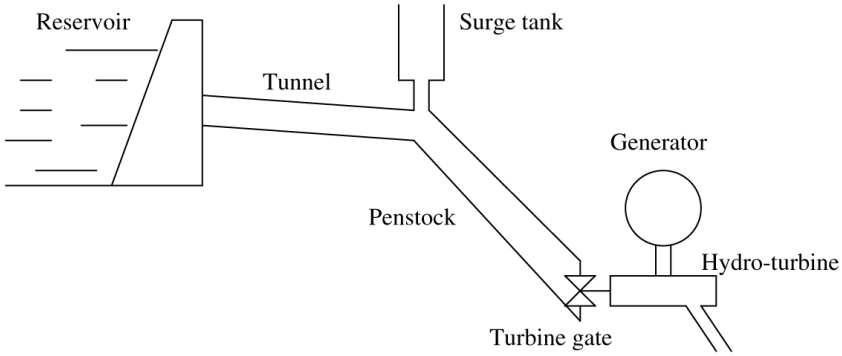

Figure 4.1 – General layout of a hydro power plant [11]

The hydro power plant dynamics is now shortly described. As seen in Figure 4.2 the speed (frequency) will affect both the turbine and the governor. The speed of the turbine and the gate position will have an influence on the flow in the conduit, which again affects the pressure at the turbine. Both the pressure and the flow will create a mechanical torque in the turbine. This, and the torque produced by the electrical load, will affect the generator through the rotor dynamics and have an impact on the frequency of the grid and the power output. The governor will sense the deviation in frequency and change the gate position to increase or decrease the flow.

4.2 Turbines

This part will take a brief look at the different turbines used in hydro power plants and how the output power of a turbine is derived.

4.2.1 The Different Turbines

There are two kinds of hydraulic turbines: impulse turbines and reaction turbines [8, 13]. The impulse turbine is better known as the Pelton turbine and is used for high heads of water, 300 meters or more. For a impulse turbine the runner is at atmospheric pressure. The total pressure drop takes place in the nozzle and all the specific energy is transformed to kinetic energy. Water jets from the nozzles hits spoon-shaped buckets on the runner and are aimed so they hit nearly tangential to provide torque. All the kinetic energy of the water is lost through the turbine.

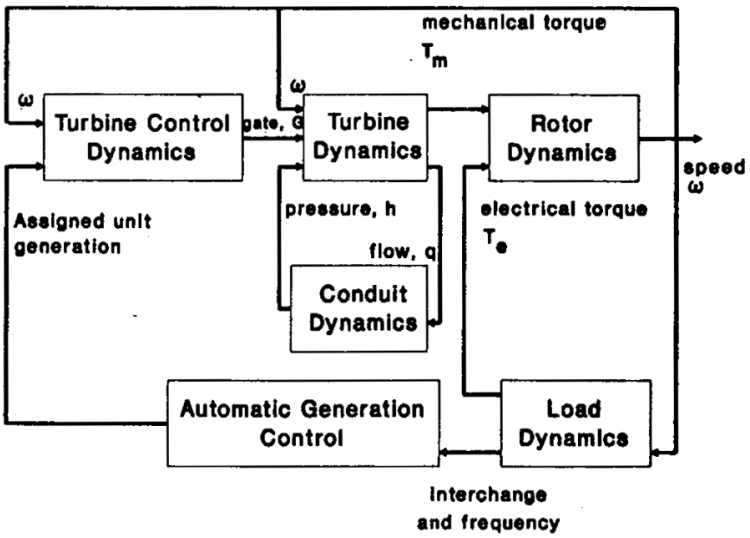

Figure 4.2 – Block diagram illustrating the relationship between the different dynamics of a hydro power plant [12]

In the reaction turbine the pressure within the turbine is above atmospheric, hence the energy is supplied both kinetically and potentially since there will be both a loss of speed and pressure through the turbine. The water is first led through a spiral casing before it passes through guide vanes into the turbine. There are two main types of reaction turbines: Francis and propeller. Francis turbines are used for heads up to 360 meters. In this kind of turbine the water flows through guide vanes and impacts the runner tangentially. The propeller turbine is used for low heads, up to 45 meters, and is a propeller with either fixed or variable-pitch blades. The variable-pitch blade turbine is commonly known as the Kaplan turbine.

Linearised Turbine Parameters

The relationship between flow, speed, gate opening and efficiency for a turbine is complex. A typical characteristic diagram (Hill chart) for a Kaplan turbine is illustrated in Figure 4.3. One way of modelling the output of the turbine is to take this Hill chart into account and linearise around an operation point. The

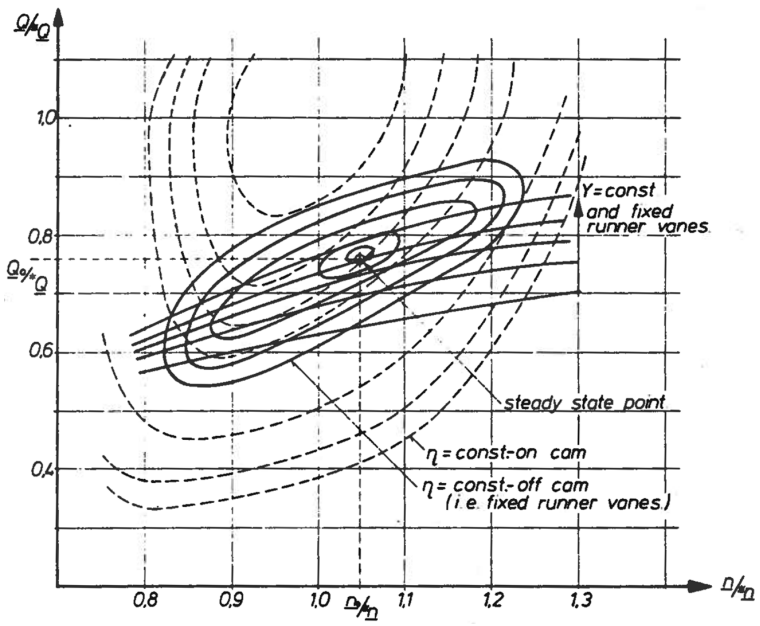

Figure 4.3 – A typical Hill chart for a Kaplan turbine [14]. n = speed, Q = flow, Y = gate opening (G) and η = efficiency

characteristic equations for this is [15]:

$$\Delta q = \frac{\partial q}{\partial n}\Delta n + \frac{\partial q}{\partial G}\Delta G + \frac{\partial q}{\partial h}\Delta h \tag{4.1}$$

$$\Delta T_{mec} = \frac{\partial T_{mec}}{\partial n}\Delta n + \frac{\partial T_{mec}}{\partial G}\Delta G + \frac{\partial T_{mec}}{\partial h}\Delta h \tag{4.2}$$

$$\Delta P_{mec} = \frac{\partial P_{mec}}{\partial n}\Delta n + \frac{\partial P_{mec}}{\partial G}\Delta G + \frac{\partial P_{mec}}{\partial h}\Delta h \tag{4.3}$$

In these equations P_{mec} - mechanical power, T_{mec} - mechanical torque, q - flow, G - gate opening and h - head. One way of using linearised turbine parameters is introduced in one of the models described later.

Hydraulic Power

For an ideal turbine the mechanical power is equal to the hydraulic power, which is the product of volumetric flow, q, and the available pressure, p [15]:

$$P = q \cdot p \tag{4.4}$$

The turbine will have a damping effect when it is operating at off nominal speed. The damping is provided with the damping coefficient D and is a function of gate opening, G and the speed deviation, Δw. The fact that the turbine is not 100% efficient is taken care of by subtracting the no-load flow q_{nl} from the actual flow. The per unit turbine power can then be expressed as [16]:

$$P_{mec} = A_T h\,(q - q_{nl}) - DG\Delta\omega \tag{4.5}$$

Here the hydraulic head, h, is used instead of the pressure. A_T is a proportional factor transforming per unit turbine power to per unit generator power and can be found with the following equation [12]:

$$A_T = \frac{\text{Turbine MW rating}}{\text{Generator MVA rating}\; h_r\,(q_r - q_{nl})} \tag{4.6}$$

Here, h_r is the per unit turbine head at rated flow and q_r is the per unit flow at rated load. The flow rate through the turbine, q, can be expressed as:

$$q = G\sqrt{h} \tag{4.7}$$

4.3 Conduit

As seen in Figure 4.2 the conduit dynamics is an important part of the total dynamic model. Some hydrodynamic theory is presented to be enable to make models for the turbine conduit system. Firstly the equations describing the inelastic water column is presented. Secondly a more detailed representation with elastic water column and surge tank is described.

4.3.1 Inelastic Water Column

The rate of change of flow in a conduit in per unit is given by [12]

$$\frac{dq}{dt} = \frac{(1 - h - h_l)}{T_w} \tag{4.8}$$

where h is defined as the head at the turbine and h_l the headloss. The water starting time T_w reflects the inertia of the water and is defined as [14]:

$$T_w = \frac{L}{A}\frac{q_{base}}{h_{base}g} \tag{4.9}$$

Here g is the acceleration of gravity and h_{base} is the static head of the water column above the turbine. L and A is the length and area of the conduit.

4.3.2 Elastic Water Column

Elasticity of steel in the penstocks and the compressibilty of water can cause a phenomenon called travelling waves or the water hammer effect [12]. This is waves of pressure and flow that can occur between the turbine and the nearest surface with atmospheric pressure, for example the surge tank [16].

If one assume a uniform conduit supplied from a large reservoir, the relationship between head and flow can be described by the following relationship [12]:

$$\frac{h\,(s)}{q\,(s)} = -Z_0 \tanh\left(T_e s\right) \tag{4.10}$$

Here Z_0 is the surge impedance of the conduit and T_e is the wave travel time. The surge impedance is defined as:

$$Z_0 = \frac{T_w}{T_e} \tag{4.11}$$

The wave travel time is related to the length of the tunnel, L, and the velocity of sound in water, v.

$$T_e = \frac{L}{v} \tag{4.12}$$

To easier model the water hammer effect Equation 4.10 can be transformed to:

$$\frac{h\,(s)}{q\,(s)} = -Z_0 \frac{\left(1 - e^{-2T_e s}\right)}{\left(1 - e^{-2T_e s}\right)} \tag{4.13}$$

4.3.3 Surge Tank

Surge tanks are used to control hydraulic transients and pressure changes [16]. The surge tank can have many different designs, but it can be described as an open chamber with atmospheric pressure located above the high pressure shaft that leads

to the turbines. It's main objective is to make the travel distance for the pressure waves occurring at the turbine shorter. In Figure 4.1 the surge tank i placed after the tunnel from the reservoir. There can also be a surge tank downstream of the turbine in the outlet tunnel. The flow through the upper tunnel, q_t, is given by:

$$q_t = q_s + q_p \tag{4.14}$$

where q_s is the flow into the surge tank and q_p is the flow to the turbines through the penstock. The surge tank flow is defined as:

$$q_s = A_s \frac{dh_s}{dt} \tag{4.15}$$

The head of the surge tank can be found by rearranging Equation 4.15 and utilizing the Laplace operator.

$$h_s = \frac{q_s}{C_s s} \tag{4.16}$$

where C_s is the surge tank storage constant and is defined as:

$$C_s = \frac{A_s h_{base}}{q_{base}} \tag{4.17}$$

The surge tank will give rise to a problem known as mass oscillations [17]. This is oscillations between the free water levels of the reservoir and the surge tank, and will have an impact on the pressure at the turbine since the pressure in the surge tank will oscillate. The frequency of the mass oscillation is given by

$$\omega_m = \sqrt{\frac{g}{A_s \frac{L_t}{A_t}}} \tag{4.18}$$

where ω_m is the frequency in rad/s, L_t is the length of the tunnel, A_t and A_s is the tunnel and surge tank cross section respectfully, g is the acceleration of gravity.

4.3.4 Head Loss

Head loss will occur because of frictional loss in the conduit. The tunnel, penstock and surge tank will have surface friction. The head loss can be found with the following equation [15]:

$$h_l = f \frac{Lq^2}{d^5 0.125 g \pi^2} \tag{4.19}$$

The variables in this equation is the frictional factor, f, and the flowrate, q. L and d is the length and diameter of the tunnel or penstock. f is not constant for transient flow, but can be set constant for good approximation.

To model the frictional losses the following equation is being used:

$$h_l = f_p q^2 \tag{4.20}$$

f_p is the frictional coefficient in per unit and is given by:

$$f_p = \frac{L}{d^5 0.125 g \pi^2} \frac{h_{base}}{q_{base}^2} \tag{4.21}$$

4.4 The Hydraulic System Models

Three models for the hydraulic system will now be presented.

4.4.1 Classical Model

The Classical model is the most common model used in power system stability studies and is presented i Figure 4.4. This is a simple non-linear model gathered from Kundur [8]. The model takes two input variables, the speed error, $\Delta\omega$, and the gate position, G, and the output is mechanical torque, T_{mec}.

The available head at the turbine is found with Equation 4.7. The rate of change of flow from Equation 4.8 is implemented with the water starting time T_w. Damping is included with the coefficient D as described in Equation 4.5. The model is non-linear due to the multiplication and division of signals. This model neglects all frictional losses and sees the water as inelastic, which means that the water is incompressible and the water hammer effect is not included.

4.4.2 The IEEE Model

This non-linear model is proposed in a paper from the *Working Group on Prime Mover and Energy Supply Models for System Dynamic Performance Studies* [12]. This is an IEEE working group dedicated to develop models for studies like those presented in this thesis. The model is presented in Figure 4.5 and will be referred

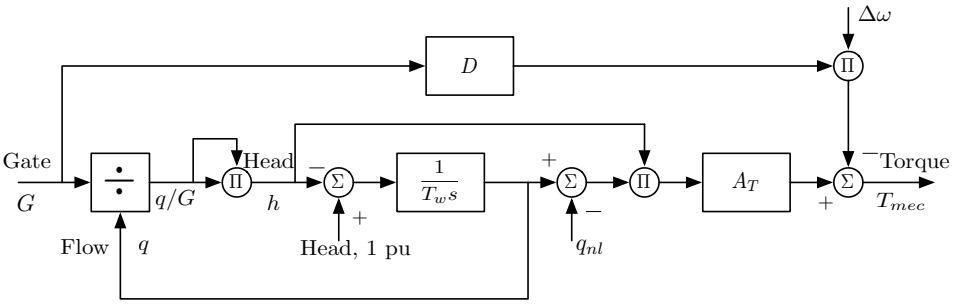

Figure 4.4 – Block diagram for the classical model [8]

to as the IEEE model. This model is also presented in the Master's Thesis of Ola Høydal Helle and Luz Alexandra Lucero Tenorio [15, 18].

This model takes the same input variables as the Classical model and the output is mechanical torque, T_{mec}. The model is based on the same fundamental equations as the Classical model, but includes the water hammer effect due to elasticity, the effect of the surge tank, and the head losses.

The model can be divided into three parts according to the placement in the block diagram of Figure 4.5; the tunnel, the surge tank and the penstock. The upper part, consisting of the water starting time T_{w2} and the frictional loss proportional to f_{p2}, is the model of the tunnel. Here, T_{w2} is the tunnel water starting time. Underneath, the surge tank is modelled with the storage time constant C_s and the head loss f_0. The penstock is modelled with the water hammer effect with the exponential loop as described by Equation 4.13. f_{p1} represents the head loss in the penstock. Damping is included with the reference for the speed deviation, $\Delta\omega$.

4.4.3 The Turbine Parameter Model

The turbine parameter model is presented in Figure 4.6 and is based upon the IEEE model. As with the IEEE model, the turbine parameter model takes the influence of water hammer, surge tank and head losses into account and is a non-linear model.

What makes this model different is that it does not use the standard turbine equation to find mechanical torque. The partial derivatives defined in Equation 4.1 and 4.2 are used to model the relationship between the different variables. In Ola's

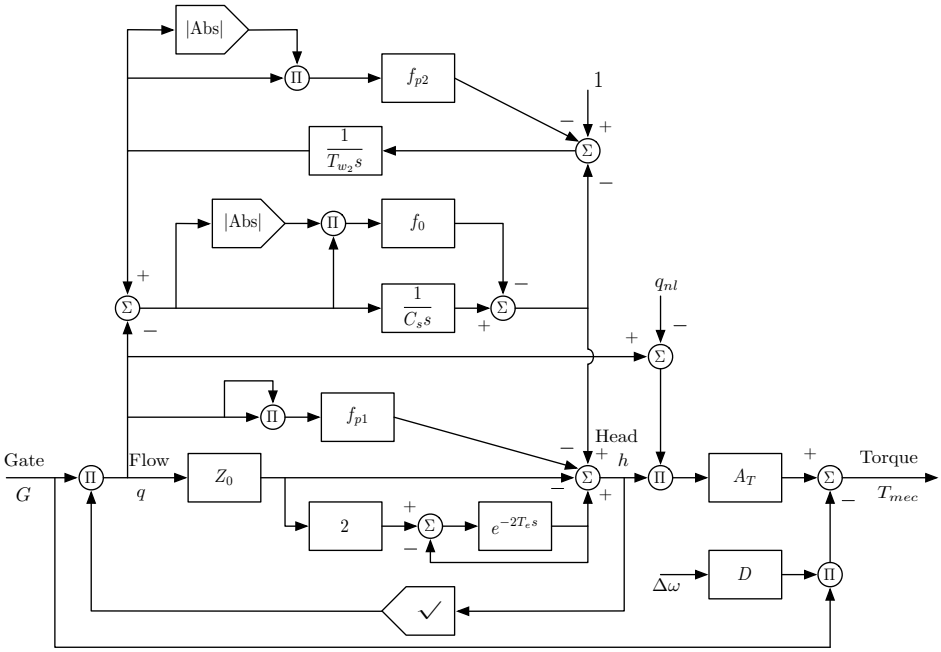

Figure 4.5 – Block diagram for the IEEE model [12]

work this gave a more accurate model, but for simulations the different partial derivatives are values that are difficult to find [15].

4.5 Comparison of the Models

The models are implemented as DSL-files to be able to use them in SIMPOW®. SIMPOW® has the ability to run independent models in order to find the frequency response. This has been done in the frequency range 0.0001 - 1 Hz. The resulting Bode-diagram is shown in Figure 4.7.

It should be mentioned that the development of models in HiDraw is complicated and that the models used in this Thesis are based upon the work of Ola Høidal Helle [15]. The turbine parameter model was not successfully implemented in the network model, but a standalone model was tested to give the response in Figure 4.7.

As seen in Figure 4.7 there is a significant difference between the classical model and the detailed models. Both of the detailed models has a phase shift of -90°

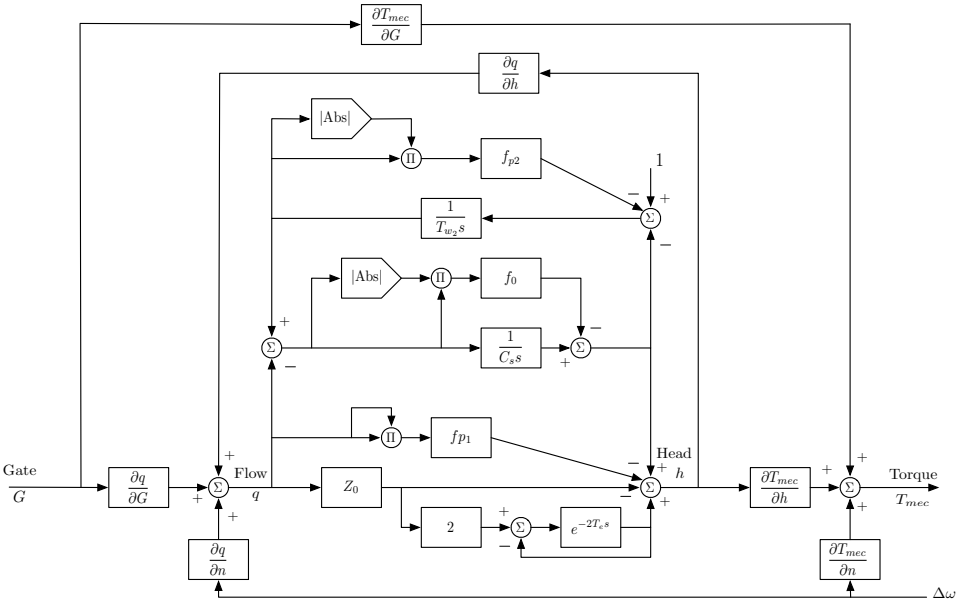

Figure 4.6 – Block diagram for the turbine parameter model [15]

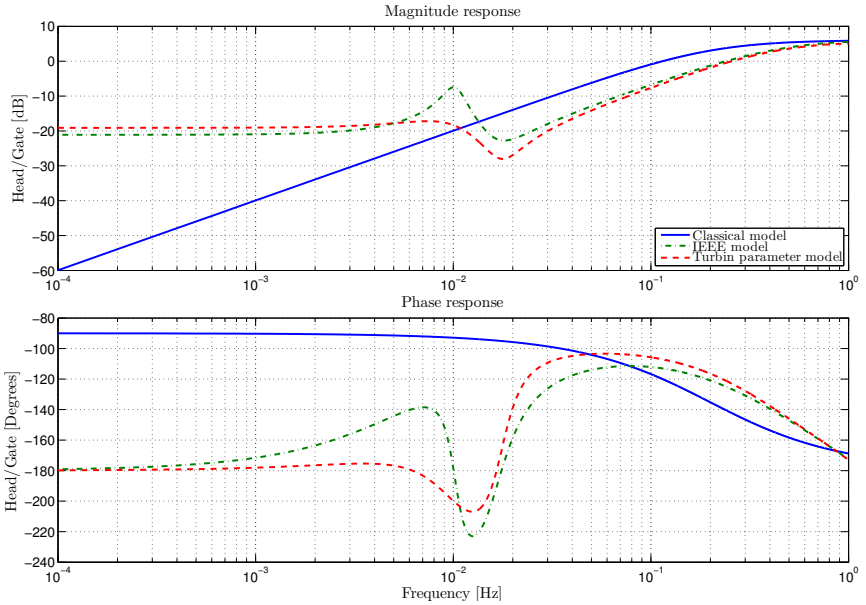

Figure 4.7 – Frequency response for the different models

from the Classical model for low frequencies. There is also a big difference in gain since both of the detailed models has a constant higher gain for low frequencies. At frequencies higher than 0.1 Hz the models have a more or less equal response, but for higher frequencies the water hammer effect will have an impact. The higher frequencies is not the scope for this Thesis.

From the bode diagram it is also observed that there is a mode present at a frequency of around 0.012 Hz for the detailed models. There is a dip in both the magnitude and phase response. This mode is a result of a very high time constant and are connected to the surge tank storage constant. [19] states that "the water level fluctuation in the surge tank causes low-frequency fluctuations of unit's output power and frequency". This will be further studied in Chapter 7.

4.6 Consequences of the Non-Linearities

Three non-linear models for the hydraulic system are presented in this chapter. They are all non-linear since they include multiplication and division of different signals. An example is the head in the Classical model which is found by taking the square of the flow divided by the gate opening ($h = (q/G)^2$).

The eigenvalue analysis was is a way of describing a large dynamic system by a set of linear combinations of different modes. For non-linear systems this is not possible with the same methods. It is possible to linearise around a specific operation point, but the eigenvalues will just be valid for this point. Small changes in one signal may cause significant changes in the eigenvalues.

DSL-code is considered as a good way of implementing non-linear systems for simulations in SIMPOW® [10], but this is difficult and for this Thesis models developed by earlier master students were used [18, 15]. With non-linear systems Dynpow will manage to do time-domain analysis, but since the eigenvalues are valid for one operation point only it is not possible to do any accurate eigenvalue analysis in form of sensitivity analysis. The eigenvalue analysis in this Thesis is therefore limited to only calculating the eigenvalues.

Chapter 5

Turbine Governing Systems

The turbine governing system is important for control of the turbine and generator output. By regulating the flow through the turbine the governor is used to control the frequency in the grid and the active power output of the generator. This chapter considers why there is a need for turbine governing systems and presents different mathematical models.

5.1 Fundamentals of Turbine Governing

Stable frequency is one of the requirements for stable operation of the power system. In the Nordic power system the frequency is 50 Hz and the Nordic Grid Code specify that it should be regulated within limits of 50±0.1 Hz [3]. For a synchronous generator the speed is directly connected to the grid frequency. The torque balance in the system is given by the difference between the driving mechanical torque from the water in the turbine and the electrical load torque. This relationship is defined by the swing equation [7]:

$$J\frac{d\omega}{dt} = T_{mec} - T_{el} \tag{5.1}$$

As a result of Equation 5.1 the system frequency and power consumption are directly connected. If the electrical load torque decrease the system will have a nett driving mechanical torque from the turbines and the frequency will increase. If the electrical power consumption is larger than the produced mechanical power the frequency will decrease. The rate of change in frequency is given by the inverse of the total inertia in the system, J. The rate of change is thereby dependent on the size of the system and the number of production units. For island operation,

operation with only one or a few generators, frequency control is a challenge since J will be smaller and the frequency variation larger.

One method of speed control is to have a feedback of the frequency deviation to the turbine governor. Stable operation of multiple units are achieved by implementing a droop characteristic which will ensure that load is shared between the different generating units. A typical droop characteristic is presented in Figure 5.1 where the slope of the curve is given by the permanent droop R_P. This type of control is called primary frequency control and several generating units are provided with primary droop in order to get the appropriate load sharing.

Automatic active reserves is a term involved in primary frequency control and is the reserves that are activated during normal operation disturbances. In other words, the reserves needed to provide primary frequency control and distribute the changes in load over several generating units.

5.2 Governing Systems for Hydraulic Turbines

Due to the special response between the water and turbine and the high forces needed to move the gate, governing systems for hydraulic turbines on hydro power plants differ from other governing systems. Since there is an inertia in the water the governor has to limit the gate movement in order to let the water flow catch up. This is provided with the transient or temporary droop feedback R_T. The purpose of this feedback is to limit the gain, and hence limit the gate movement, for a time given by the reset time constant T_R.

Today there is two main types of governors. The one that is used at old powerstations is the mechanical-hydraulic governor, but at new installations it is more common to use an electrohydraulic governor. The principal is the same for both of them and they will now be explained more in detail.

5.3 Mechanical-Hydraulic Governor

For the mechanical-hydraulic governor the speed sensing device is mechanical. The computing functions and permanent droop feedback are provided with mechanical components. Functions that are more power demanding, such as the gate

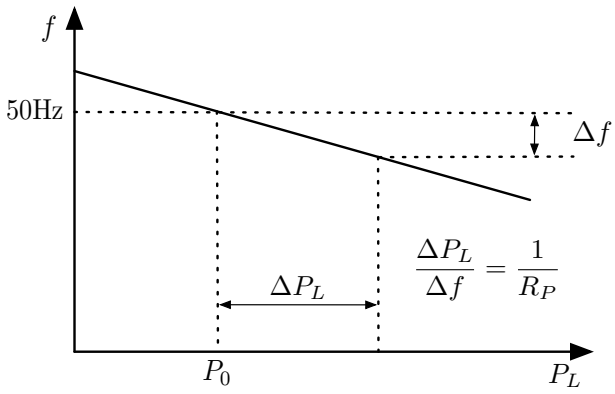

Figure 5.1 – The droop characteristic. R_P is the permanent droop

movement, are achieved by hydraulic components. Figure 5.2 shows a simplified schematic of a mechanical-hydraulic governor [20].

The mechanism used is called the Watt centrifugal mechanism [7]. A set of flyballs is driven by the turbine shaft and the height of the flyballs depends on the speed. If the electrical torque equals the mechanical torque the speed of the shaft is constant and the height of the flyballs do not change. If there is a difference in torque, the shaft will accelerate or decelerate, and the position of the flyballs will change. This will affect the pilot valve servo which in turn will make the gate servomotor move the gate. The transient droop is achieved with a compensating dashpot.

5.3.1 Mathematical Representation

One classical way of modelling the mechanical-hydraulic governor is presented in Kundur, and will be referred to as the Classical governor [8]. The block diagram for this model can be seen in Figure 5.3.

This model has both the transient droop R_T, which is a result of the compensating dashpot, and the permanent droop R_P. The permanent droop is the part of the governor that makes sure that the load is shared by different power plants. For steady state the governor output, the gate opening, is given by:

$$\Delta G = \frac{1}{R_P}\Delta w \tag{5.2}$$

For fast changes in frequency, for example when a large load is disconnected, it is

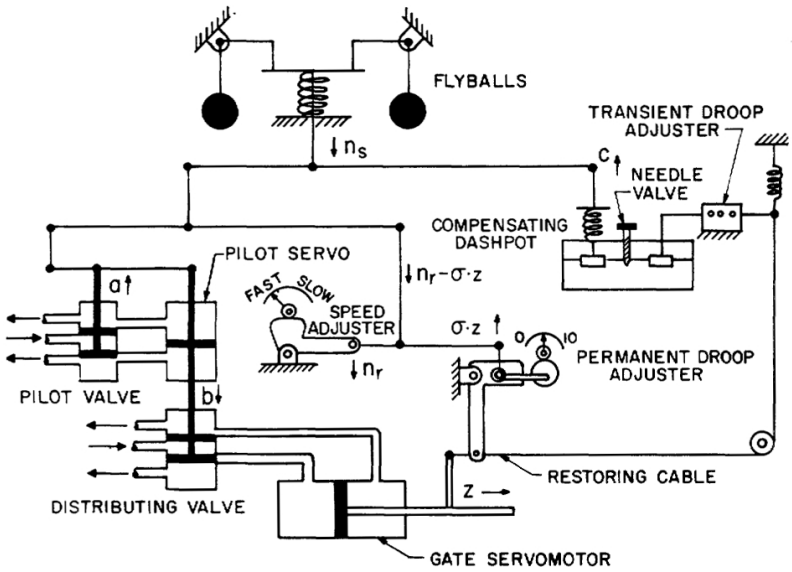

Figure 5.2 – Mechanical-hydraulic governing system [20]

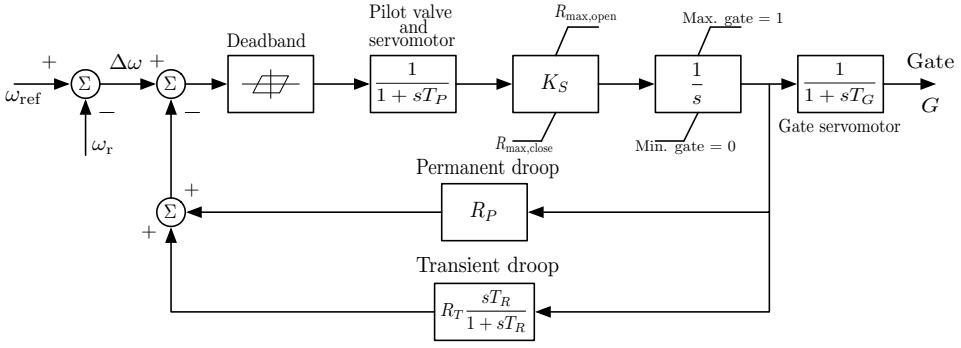

Figure 5.3 – Block diagram for the Classical governor [8]

desirable to have a lower gain. This is due to the fact that the turbine may have to change it's power output significantly and the water has high inertia which makes it slow to regulate. This is achieved by the temporary droop R_T and the reset time constant T_R.

$$\frac{\Delta G}{\Delta w} = \frac{(1+sT_R)}{\frac{T_R T_G s^4}{K_S} + \frac{(T_G+T_R)}{K_S}s^3 + \frac{(1+K_S R_T T_R T_G)}{K_S}s^2 + (R_P T_G + R_T T_R)\,s + R_P} \tag{5.3}$$

The gate pilot valve and servo motor is modelled as delays with the time constants T_P and T_G respectfully. T_P is usually much smaller than T_G and can be neglected. With T_P set to zero, the complete transfer function will be given by Equation 5.3. For steady state ($s = 0$) this equation will be equal to Equation 5.2.

5.3.2 Illustration

An example is made to illustrate the effect of the temporary droop and the reset time constant [12]. The magnitude response of two simplified governors can be seen in Figure 5.4. In this example the time constants of the servo motors has been set to zero. The steady state gain is $20\log(1/R_P) \approx 57$. The frequency at which the gain is settling at a lower value of $1/R_T$ is given by $1/T_R$. For T_{R2} this frequency will be 1/5=0.2 Hz, which corresponds to 1.26 rad/s in Figure 5.4. The gain at this frequency will be approximately $20\log(1/R_T)$. In Figure 5.4 its easy to see that a higher T_R means that the gain will start to decrease at lower frequencies. Both the magnitude and phase response are shifted towards lower frequencies.

As illustrated in Figure 5.3 the temporary droop and the reset time is closely connected, and an example showing variation of R_T is presented in Figure 5.5. In this example the reset time is equal, so the frequency where the magnitude settles are equal for both settings. By increasing R_T the gain at higher frequencies will be lower. Similarly as for higher T_R another impact of increased R_T is that the gain will start to decrease for lower frequencies.

5.4 Electrohydraulic Governor

As mentioned earlier is it common to install the more modern electrohydraulic governor at new hydro power stations. Their functionality is very similar to that of mechanical-hydraulic governors, but the speed sensing, permanent droop

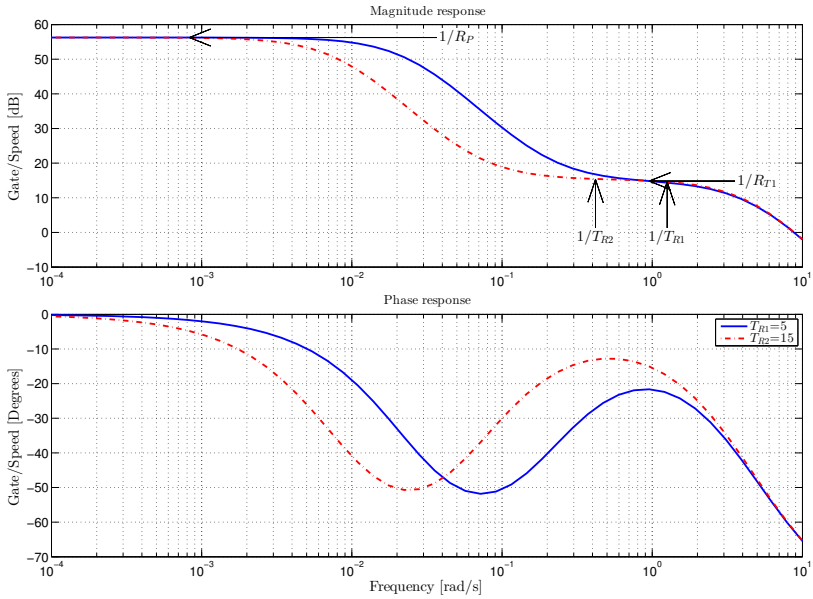

Figure 5.4 – Frequency response for a governor with different values for T_R. K_S=10, R_T=0.4 and R_P=0.06. The horizontal arrows indicate amplitude values and the vertical arrows indicate frequencies

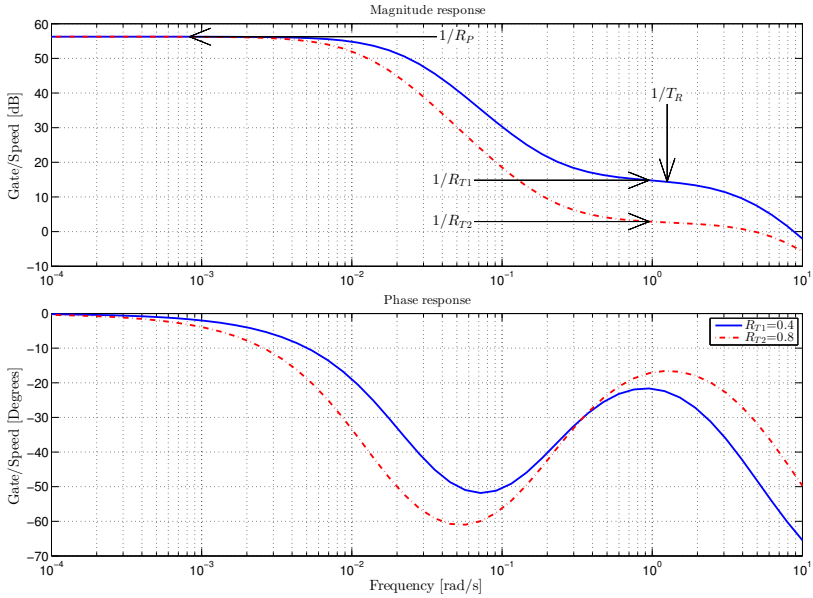

Figure 5.5 – Frequency response for a governor with different values for R_T. K_S=10, T_R=5 and R_P=0.06. The horizontal arrows indicate amplitude values and the vertical arrows indicate frequencies

and computing functions are performed electronically [20]. The electrohydraulic governor uses the same hydraulic components as the mechanical-hydraulic for the power demanding tasks. An advantage with the electric components is that they provide more flexibility regarding time delays and dead bands.

5.4.1 Mathematical Model

The electrohydraulic governor is built up as a PID controller, which means that the signal fed to the pilot servo is a combination of a proportional, derivative and integral term. The simple PID governor is shown in Figure 5.6. The big difference between this model and the Classical model is that there is no transient droop feedback. The transient droop can be implemented by adjusting the different gains; K_P - proportional gain, K_I - integral gain, K_D - derivative gain.

The transfer function for the PID governor is described by Equation 5.4. This equation fulfils the criterion described by Equation 5.2 for steady state.

$$\frac{\Delta G}{\Delta w} = \frac{1}{R_P} \frac{K_D s^2 + K_P s + K_I}{K_D T_G s^3 + \left(K_D + T_G\left(K_D + \frac{1}{R_P}\right)\right)s^2 + \left(K_P + K_I T_G + \frac{1}{R_P}\right)s + K_I} \tag{5.4}$$

5.5 Comparison of the Models

A frequency response plot has been made for the models described in this chapter. This is presented in Figure 5.7. The parameters used is listed in Table A.10 and A.11 in Appendix A. As seen in Figure 5.7 the response for the

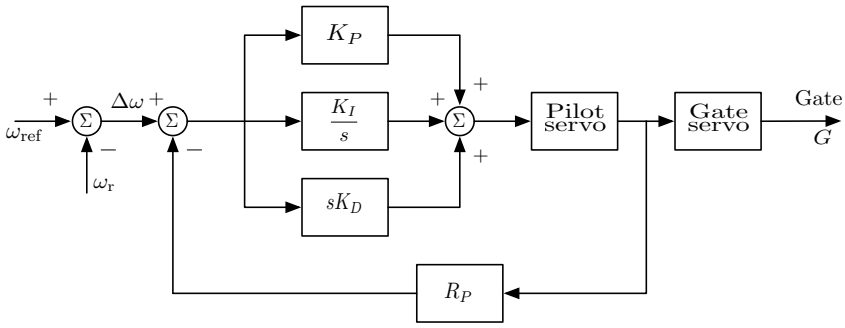

Figure 5.6 – Block diagram for the PID governor [8]

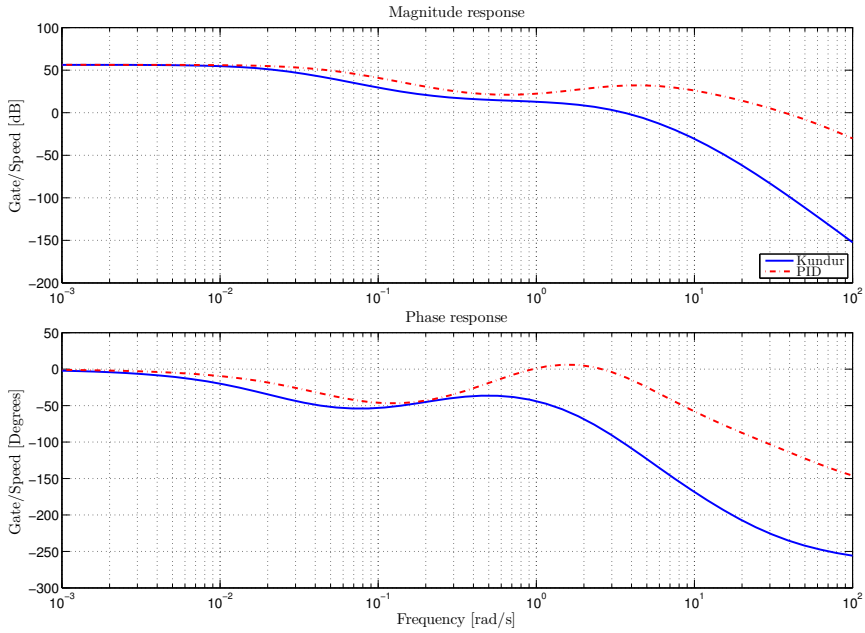

Figure 5.7 – Frequency response for the different governor models

PID governor is similar to the Classical governor for low frequencies. The transient droop is therefore successfully implemented by choosing correct values for the proportional and integral gain. The reason for the new peak in the frequency response at around 2 Hz is the derivative term of the governor. For this governor the derivative gain is quite high and may not be particularly good tuned, but it is just made to illustrate the effect of the derivative term in the control loop.

5.6 Recommendations

In Chapter 9 in Kundur's *Power System Stability and Control* a way of tuning the governor is described [8]. The choice of R_T and T_R are related to the water starting time T_w and the mechanical time constant T_M. The optimum choice is described as follows:

$$R_T = [2.3 - (T_w - 1.0)0.15]\frac{T_w}{T_M} \tag{5.5}$$

$$T_R = [5.0 - (T_w - 1.0)0.5]T_w \tag{5.6}$$

Suggestions for the tuning of the PID governor parameters was presented in Luz Alexandra Lucero Tenorio Thesis [18]. The following equations will give the optimum values for the parameters:

$$K_P = 0.8\frac{T_M}{T_w} \tag{5.7}$$

$$K_I = 0.24\frac{T_M}{T_w^2} \tag{5.8}$$

$$K_D = 0.27T_M \tag{5.9}$$

The parameters used for simulations in SIMPOW® are presented in Table A.10 and A.11 in Appendix A. The optimal parameters for the water conduit and turbine presented in the same appendix in Table A.12.

Chapter 6

Reduced System Model

For analysis in SIMPOW® there is need for both a Optpow and a Dynpow file. The Optpow file is, as earlier described, where the network topology is defined for doing optimal power flow analysis. The Dynpow file describes the dynamics of the different sub-systems such as generators, turbines and governors. The reduced system model is a three-machine equivalent of the Norwegian ans Swedish power system and will be presented in this chapter.

6.1 Model for Optimal Power Flow

The model comprise three areas that will represent Norway and Sweden, where Sweden is modelled with two areas. The area corresponding to the production in Norway will be modelled with 100% hydro power. Sweden has almost 50% hydro power and 50% nuclear power, hence the two areas representing Sweden are modelled with equal amount of power but one area has been set to have constant power output and no primary control [21]. The model is illustrated in the simple one-line diagram in Figure 6.1.

The areas are connected with three lines where each line represents five parallel triplex 420 kV lines. The areas are loaded so that there is a surplus of power in Norway and the flow of power goes from Norway to Sweden. A power injection of 1 600 MW is added to the bus representing Norway to easily simulate a generating loss equal to the dimensioning fault in the Nordic power system. The parameter values used can be found in Table A.1 in Appendix A. The power system is described in an Optpow file to be used in SIMPOW® for optimal power flow analysis and can be found in Appendix B. The result of the optimal power flow is presented in a one-line diagram in Appendix C.

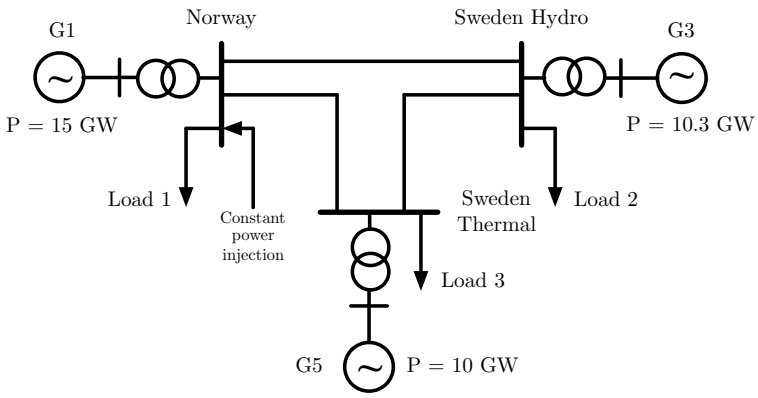

Figure 6.1 – Simplified one line diagram for the reduced system model

6.2 Models for the Dynamic Analysis

To be able to do dynamic analysis in SIMPOW® a Dynpow file, which include the different dynamic sub-systems and parametrization of these, have to be made. The different dynamic sub-systems are here briefly explained. The Dynpow file used in the case study can be found in Appendix D.

6.2.1 Excitation System and Power System Stabilizer

Since there is a constant change in the power output of the generator, due to constant change in load, there will be a change of current and voltage at the terminal of the generator. The basic requirement for the excitation systems is to automatically adjust the field current of the synchronous generator to maintain the required output voltage at the terminal of the generator [8]. There are several methods to do this, and the method used in the reduced system model is gathered from the *Kundur Two-Area System* where a thyristor controlled high gain exciter is implemented [22]. This can be seen in Figure 6.2 and will be used in the reduced system model.

In many situations the excitation system is unstable and poorly damped oscillations can occur. The power system stabilizer uses auxiliary signals to control the excitation system [8]. In Figure 6.3 the signal used is the grid frequency, but other signals can be power and prime mover speed. The power system stabilizer are meant to provide better damping to the system oscillations and enhance the

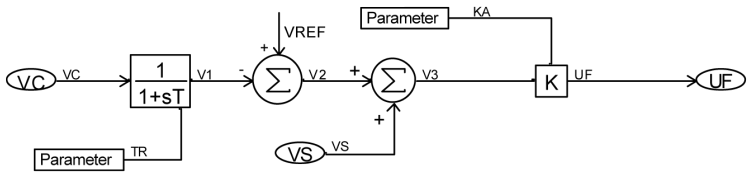

Figure 6.2 – Thyristor exciter with high gain [22]

stability. The PSS shown in Figure 6.3 is also gathered from the *Kundur Two-Area System* and will be used in the reduced system model together with the exciter in Figure 6.2.

Both the excitation system and the power system stabilizer is necessary to get a stable power system. The models will not be explained further since it is not the goal of this Thesis. Parameter values used for the exciter and PSS can be found in Table A.5 and A.6 in Appendix A.

6.2.2 Synchronous Generators

There are three synchronous machines in the system. Two of them, G1 and G3, are used to simulate the effect of hydro power plants, and are equipped with hydraulic systems and governors. The third, G5, is used as a constant input and is not a part of the primary reserve.

There are several synchronous machines implemented in SIMPOW®, the one used here is the TYPE 1, which is the most detailed model. This model includes one field winding, one damper winding in d-axis and two damper windings in q-axis and is a sixth-order model [10]. The sixth-order model is described in *Power System Dynamics Stability and Control* and will be shortly described here [7]. This model

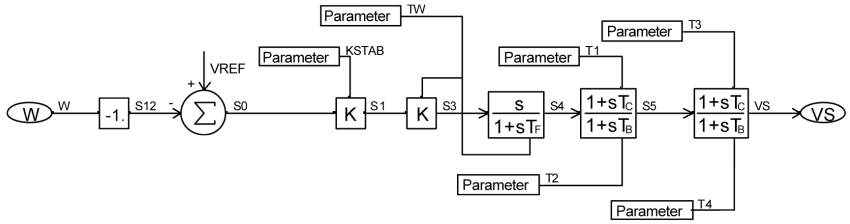

Figure 6.3 – Power system stabilizer [22]

is defined by the following equations:

$$M\Delta\dot{\omega} = P_{mec} - P_{el} \tag{6.1}$$

$$\dot{\delta} = \Delta\omega \tag{6.2}$$

$$T'_{d0}\dot{E}'_q = E_f - E'_q + I_d\left(X_d - X'_d\right) \tag{6.3}$$

$$T'_{q0}\dot{E}'_d = -E'_d + I_q\left(X_q - X'_q\right) \tag{6.4}$$

$$T''_{d0}\dot{E}''_q = E'_q - E''_q + I_d\left(X'_d - X''_d\right) \tag{6.5}$$

$$T''_{q0}\dot{E}''_d = E'_d - E''_d + I_q\left(X'_q - X''_q\right) \tag{6.6}$$

Equation 6.1 and 6.2 is the swing equations and are added to include the speed deviation and the change of the rotor angle. For this model the generator is represented by the subtransient emfs E''_q and E''_d behind the subtransient reactances X''_d and X''_q defined by this equation:

$$\begin{bmatrix} V_d \\ V_q \end{bmatrix} = \begin{bmatrix} E''_d \\ E''_q \end{bmatrix} - \begin{bmatrix} R & X''_q \\ -X''_d & R \end{bmatrix} \begin{bmatrix} I_d \\ I_q \end{bmatrix} \tag{6.7}$$

The power of the generator is given by:

$$P_{el} = \left(E''_d I_d + E''_q I_q\right) + \left(X''_d - X''_q\right) I_d I_q \tag{6.8}$$

The four Equations 6.3-6.6 describes the change of the emfs presented in Equation 6.7. All these equations are related to what was earlier presented as the rotor dynamics. The parameter values used in the simulations are given in Table A.4 in Appendix A.

6.2.3 Hydraulic System

Different models for the hydraulic system were presented in Chapter 4. For the case studies the Classical (Figure 4.4) and the IEEE model (Figure 4.5) has been chosen for further study. The Classical model lacks the effect of the water hammer and the surge tank but is used to represent the models implemented in power system analysis tools. The IEEE model is chosen as the more detailed model, this i due to the problems with the implementation of the Turbine Parameter model.

Parameters for a hydro power plant are gathered from the IEEE paper that

presented the IEEE model [12], and are given in Table A.7 in Appendix A. The parameters used for the model in the case study are derived from these values with the Equations established in Chapter 4 and are given in Table A.8. The calculation of the parameters are presented in Appendix E.

6.2.4 Governing System

The different governing systems were presented in Chapter 5 and the model that will be used in the case studies are the Classical model (Figure 5.3). Due to the fact that the PID governor can be tuned to have the same response as the Classical governor for low frequencies, and that the higher frequencies are beyond the scope of this Thesis, the PID governor will not be studied further.

The parameter values used for the study is found in *Power System Stabilty and Control* and are standard values [8]. They are presented in Table A.10 in Appendix A.

Chapter 7

Case Study

This chapter will present a case study with the intention of finding out what causes the low-frequency oscillations

7.1 Introduction to the Case Study

The reduced system model was established in the previous chapter and will be used in the case study. To illustrate the dynamic behaviour simulations with disconnection of the 1 600 MW power injection in Norway are performed. The eigenvalues has been studied to some extent.

Case A will present an analysis of the different hydraulic models and how they affect slow floating in grid frequency. The dynamic response are presented for both the Classical and IEEE model.

In Case B the impact of turbine governor parameters are studied by doing simulations with variation of one parameter at the time. The Classical governor has been used in this analysis.

The goal for Case C was to see what happens if the generators are equipped with different hydraulic models, which is the case for the real power system.

During the two last weeks of the work on this Thesis more insight in the IEEE model was obtained. It was discovered that the tunnel and penstock frictional coefficients were mixed up and that the value for T_{w2} was set to be equal T_w. It is therefore important to notice that for Case A, B and C T_{w2}=1.604, f_{p1}=0.0372 and f_{p2}=0.0112, and not the values presented in Table A.8 in Appendix A. This will be explained further in Case D.

7.2 Case A: Impact of Different Hydraulic Models

For this case the main motivation was to find out if there are any differences in the response with detailed modelling of the hydraulic system and if detailed modelling can cause slow floating in the grid frequency.

7.2.1 Comparison of the Models

For this test the system was represented by the reduced system model and the Classical governor model was used with the parameter values listed in Table A.10. Both the regulating generators were equipped with the same hydraulic model and governor. The linear analysis tool in SIMPOW® was first used to compute the eigenvalues for the system and the eigenvalues with an imaginary part lower than 1 Hz are presented in Table 7.1 and 7.2.

As seen in Table 7.1 the Classical model has two low-frequency modes, but both have relatively good damping since the damping ratio is above 50%. The IEEE model however has two modes with frequency around 10.1 mHz, which can be seen in Table 7.2. They are both poorly damped compared to the the other eigenvalues.

To illustrate the effect of the modes found in the linear analysis a dynamic analysis was carried out in SIMPOW®. After 5 ms the 1 600 MW power injection at the bus representing Norway was disconnected to simulate a loss of power production. The simulation were done for both the Classical and the IEEE model and the results are presented in Figure 7.1.

As seen in Figure 7.1 the responses are similar in the way that they almost swing towards the same steady state value. The Classical model reach a new steady state value after 180 seconds, while the IEEE model starts to oscillate around a slightly lower steady state value. The difference in steady state frequency is caused by

Table 7.1 – Eigenvalues for the system with the Classical model

Number	**Eigenvalue** Real part [1/s], Imaginary part [Hz]	**Damping ratio**
$\lambda_{Classical,1}$	$-0.507910 \pm j0.027519$	94.66%
$\lambda_{Classical,2}$	$-0.025681 \pm j0.006079$	55.80%

Table 7.2 – Eigenvalues for the system with the IEEE model

Number	**Eigenvalue** Real part [1/s], Imaginary part [Hz]	**Damping ratio**
$\lambda_{IEEE,1}$	$-0.342910 \pm j0.030471$	87.31%
$\lambda_{IEEE,2}$	$-0.003794 \pm j0.010144$	5.94%
$\lambda_{IEEE,3}$	$-0.005318 \pm j0.010127$	8.33%

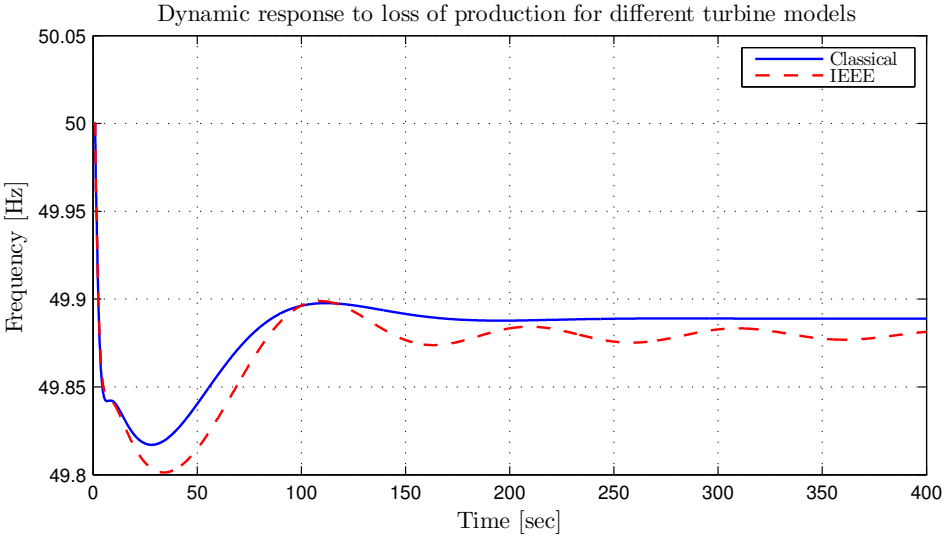

Figure 7.1 – Dynamic response to loss of production for different turbine models

the included head losses in the IEEE model. The oscillation is poorly damped and the frequency is measured to be around 10.2 mHz, which corresponds to the value of imaginary part of the eigenvalues $\lambda_{IEEE,2}$ and $\lambda_{IEEE,3}$. If one look at the bode diagram for the different models in Figure 4.7 in Chapter 4, the frequency of oscillation also corresponds with the peak and dip in the phase and amplitude response for the IEEE model. To make the bode diagram in Figure 4.7 the same parameter values were used as in Case A, B and C.

By measuring the peaks of the oscillation the relative damping can be found from a time response by using Equation 2.10. From Figure 7.1 the difference between peak 2 and 3 were measured and the damping ratio was found to be 3.5%, which is a bit lower than the damping found by eigenvalue analysis.

7.2.2 Analysing the IEEE Model

The next step was to identify what's causing this low-frequency oscillation. [23] states that "the water level fluctuation in surge tank causes low-frequency fluctuations of unit's output power and frequency, which adversely affect the response of hydro turbine governing system", hence the impact of the surge tank is of great interest. In Chapter 4 the mass oscillation was introduced as a drawback with the surge tank [19, 17].

With the parameter values for the hydro power plant listed in Table A.7 in Appendix A the mass oscillation frequency can be found with Equation 4.18. In this case ω_m=5.6 mHz, which is almost half the frequency of the oscillation found in Figure 7.1. The reason for this difference is that the value of T_{w2} was set equal T_w, which will be explained more in detail in Case D.

For the IEEE model used in this Thesis the surge tank is modelled with the storage time constant C_s. Because of rapid changes in the flow the water level in the surge tank will start to fluctuate and cause mass oscillations between the surge tank and the reservoir. These oscillations will affect the pressure in the surge tank which in turn cause pressure oscillations at the turbine. As illustrated in the block diagram of Figure 4.5 the power output of the turbine is given by multiplying the head, h, with the flow, q. The response of the head and flow is given in Figure 7.2 and supports the theory of pressure oscillations and the impact it will have on the frequency. In Figure 7.2 the same parameter values were used for the IEEE model as for the simulation in Figure 7.1.

Friction coefficient, f_{p2}

The mass oscillation will occur between the reservoir and surge tank, hence the influence of the friction coefficient in the tunnel, f_{p2} is of interest. The value for the friction coefficient f_{p2} was changed to observe the effect on the low-frequency oscillations and the result is presented in Figure 7.3a. The amplitude of the oscillation will be lower with increased f_{p2}, and with a value of 0.025 the oscillation has almost disappeared.

A plot with longer time scale illustrating the response of the head at the turbine is given in Figure 7.3c, which makes it easier to see the effect on the damping. From this figure it is seen that the friction coefficient has an impact on both the damping and the steady state value of the head at the turbine. With increased f_{p2} the

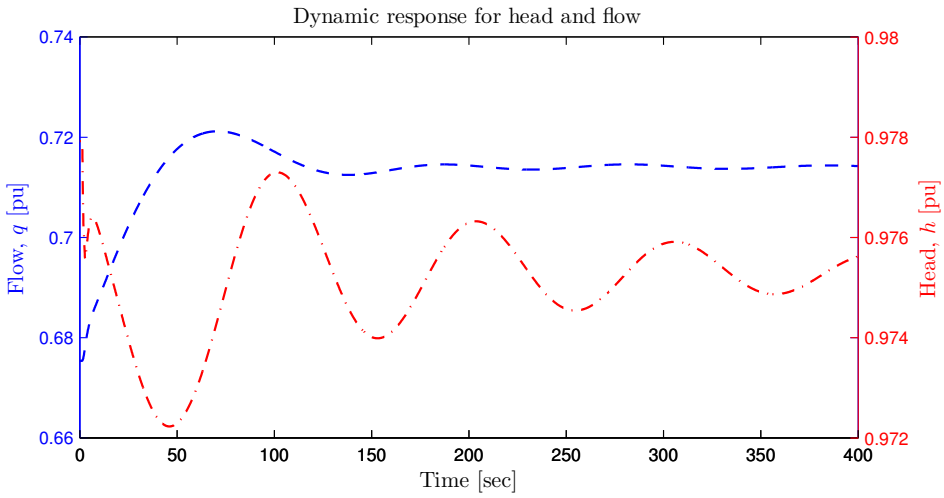

Figure 7.2 – Response in head and flow at the turbine of the IEEE model

head loss will be larger, hence the head at turbine will decrease. The oscillations disappears earlier which indicates improved damping.

Surge tank time constant, C_s

An analysis was also done to see how the surge tank time constant impacts the frequency of the oscillation. The value of C_s depends on the area of the surge tank and a larger surge tank gives a higher time constant. To easily see the oscillation the simulations were done with f_{p2}=0.005. The result is shown in Figure 7.3b, and it is observed that a higher time constant gives a lower frequency. The time period of the oscillation increase with larger surge tank.

New Eigenvalues

The eigenvalues were found with f_{p2}=0.025 and are presented in Table 7.3. From the table it can be seen that the first eigenvalue is unchanged, hence this mode has nothing to do with the oscillations in the water conduit. The two eigenvalues corresponding to the mass oscillations are now better damped due to the change in f_{p2}, which corresponds with the observation illustrated in Figure 7.3c.

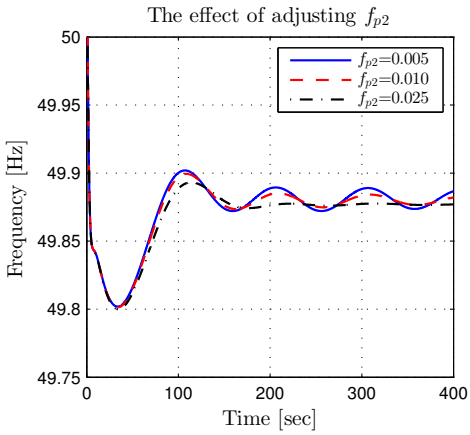

(a) Effect of adjusting f_{p2}

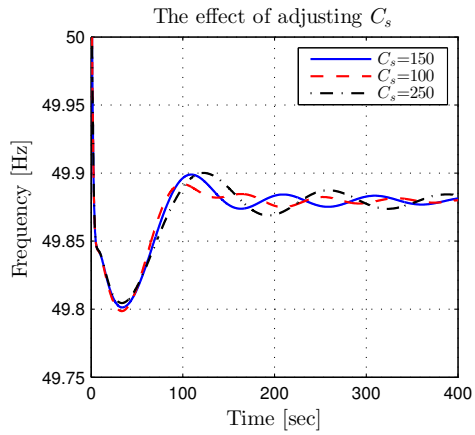

(b) Effect of adjusting C_s

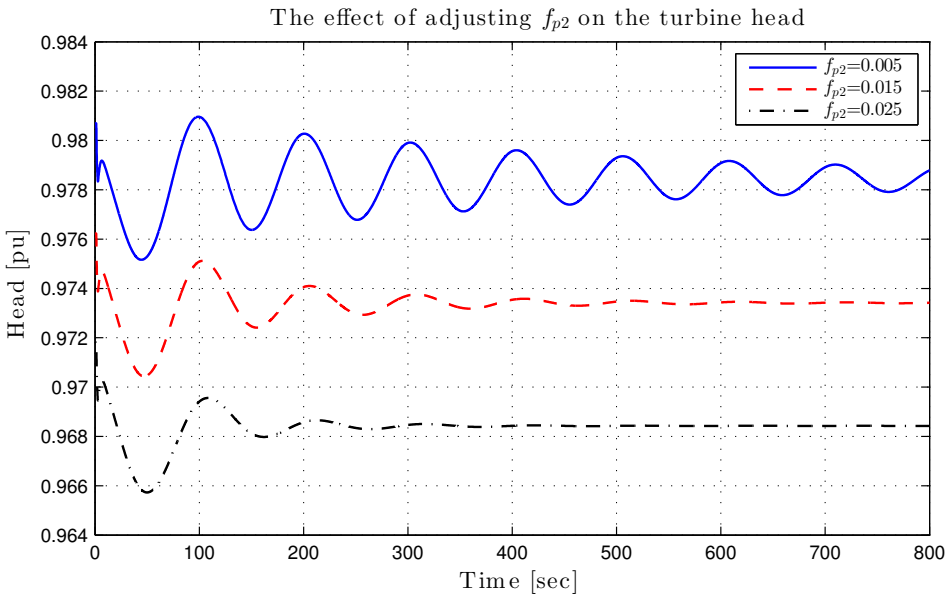

(c) Effect of adjusting f_{p2} on the response of the head h

Figure 7.3 – Dynamic response for different parameter values

Table 7.3 – Eigenvalues for the system with the IEEE model and f_{p2}=0.025

Number	**Eigenvalue** Real part [1/s], Imaginary part [Hz]	**Damping ratio**
$\lambda_{IEEE,N1}$	$-0.342950 \pm j0.030474$	87.31%
$\lambda_{IEEE,N2}$	$-0.007826 \pm j0.010096$	12.24%
$\lambda_{IEEE,N3}$	$-0.011111 \pm j0.010031$	17.36%

7.2.3 Findings

Case A has shown that there is a big difference in the models being used for the hydraulic system. The Classical model, which is the common model used in power system stability studies, lacks the effect of the surge tank. With the IEEE model the surge tank will cause mass oscillation between the surge tank and the reservoir which affects the grid frequency.

In this case a connection between the surge tank time constant, the friction coefficient in the tunnel and the frequency in the grid has been found. Both the frictional coefficients and the surge tank time constant depends on the construction of the hydro power plant. It has been illustrated that the friction coefficients has influence on the damping of the low-frequency oscillations, and the frequency of this oscillation depends on the surge tank time constant.

7.3 Case B: Classical Governor

In Case A it was shown that mass oscillations in the hydraulic system can cause low-frequency oscillations in the grid frequency. In this case the focus will be to find out if different parameters of the Classical governor can improve the damping of these oscillations. The basic parameter values are the same as for Case A with the IEEE model.

7.3.1 Dynamic Response

There is three parameters that can be tuned in the Classical governor model: R_T, T_R and R_P. If one look at the Classical model as an mechanical-hydraulic governor, the other constants are limited to actual time delays in the system and since they are very small they will only have an impact on oscillations at higher frequencies.

In this section different simulations were done to find out how the different parameters influence the dynamical response for the frequency. The parameters found in Table A.10 was used as a basis. Different plots are developed to show the impact of only one parameter at the time.

Reset time, T_R

First, the impact of the governor reset time T_R was tested. The temporary droop R_T is fed back with a time delay equal to the reset time. As seen in Figure 7.4a the response is faster with lower reset time in the way that the low-frequency oscillations starts earlier. This is as expected since this is the time constant of the feedback loop. For T_R equal 5 and 10 the response is slower and the first fluctuation will have a larger amplitude.

In Chapter 5 the frequency response of a governor was shown in Figure 5.4. It was illustrated that a higher value for T_R will cause a decrease in gain for the frequency range 0.01-0.1 rad/s, which correspond to the frequency of the oscillation in Figure 7.4a. The reason for the slower response with higher T_R is the decrease in gain. It is worth noticing that the low-frequency oscillation related to the surge tank is still intact and the variation of T_R has little or no influence on the damping.

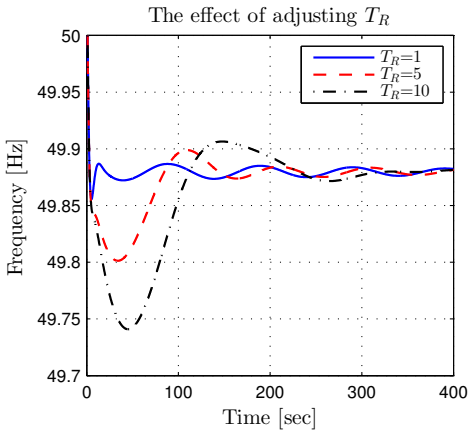

(a) Variation of T_R

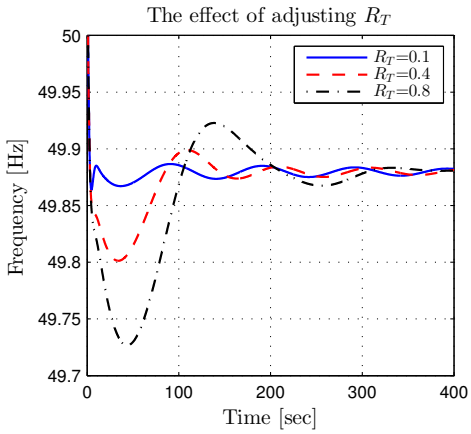

(b) Variation of R_T

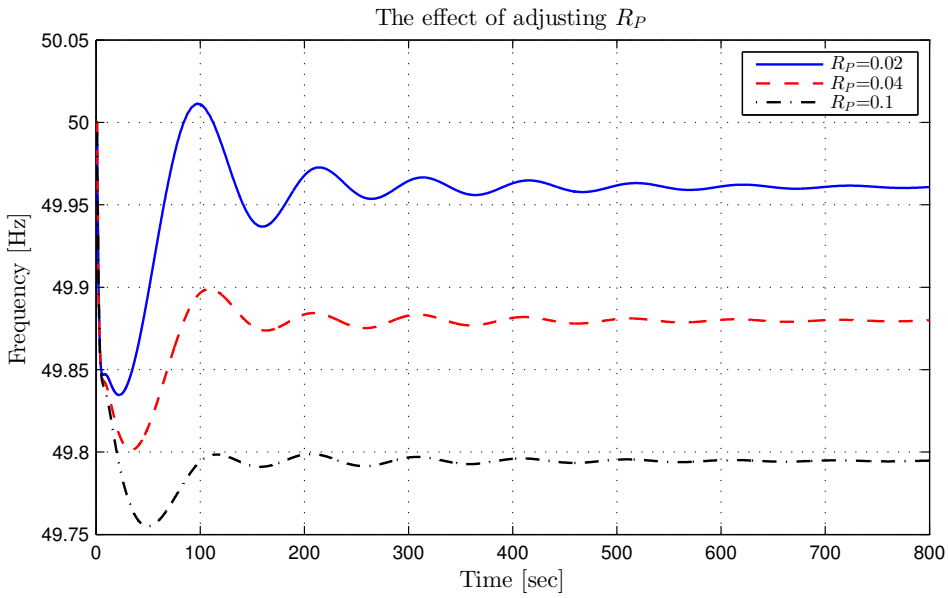

(c) Variation of R_P

Figure 7.4 – Effect of variation of the governor parameter values

Temporary droop, R_T

The temporary droop is connected with the reset time constant as seen in Figure 5.3, where R_T is multiplied with T_R to give the feedback gain. In Chapter 5 it was shown that the effect of increasing R_T is much the same as increasing T_R (see Figure 5.5). The gain for the frequency of the mass oscillations will be lower with increased R_T. The similarities are also illustrated in Figure 7.4b where the first swing will have a larger amplitude and the response will be slower for higher R_T. The low-frequency oscillation is still present and poorly damped.

Permanent droop, R_P

The impact of varying the permanent droop can be seen in Figure 7.4c. As one would expect, the permanent droop has impact on the steady state frequency in the system. With R_P=0.02 the steady state frequency deviation is smaller than with R_P=0.1, and this is how permanent droop is defined (Figure 5.1). In Figure 7.4c it is illustrated that the amplitude of the low-frequency oscillation is a little lower with higher R_P. The reason for this is that the gain will decrease with higher R_P.

In Figure 7.4c the response are plotted for t = 0-800 seconds to illustrate how poor the damping is. After 800 seconds it is still possible to see the oscillation, and this is also the case for the other plots presented earlier in the case study. The damping is not improved by adjusting R_P.

7.3.2 Eigenvalue Analysis

With variation of T_R and R_T it was shown that the response will be slower and the amplitude of first fluctuation larger for higher values of T_R and R_T. There was no indication of improved damping from the plot the of the responses in Figure 7.4. To find out if the damping was improved the eigenvalues for R_T=0.8 was found and presented in Table 7.4.

If one compare the eigenvalues in Table 7.4 with the ones in Table 7.2 there is almost no change. The eigenvalues with R_P=0.1 was also calculated and they showed more or less the same as the eigenvalues found in Table 7.4. This indicate that the governor parameters will have little impact on the damping, which supports the results from the dynamic simulations

Table 7.4 – Eigenvalues with R_T=0.8

Number	**Eigenvalue** Real part [1/s], Imaginary part [Hz]	**Damping ratio**
$\lambda_{B,TR1}$	$-0.352110 \pm j0.030477$	87.91%
$\lambda_{B,TR2}$	$-0.003752 \pm j0.010150$	5.87%
$\lambda_{B,TR3}$	$-0.005275 \pm j0.010137$	8.25%

7.3.3 Findings

In this case it has been shown that the governor parameters will have an impact on the dynamic response of the frequency in the grid. With higher transient droop and reset time the magnitude and gain response will be shifted towards lower frequencies which cause lower gain for the frequency associated with the mass oscillation. This leads to a slower response and a higher amplitude for the first fluctuation.

With variation in permanent droop the steady state frequency will change, which supports the concept of the droop characteristic. The gain will decrease with an increase in permanent droop and it has been illustrated that this will cause smaller amplitude for the low-frequency oscillation. However, the damping of the low-frequency oscillation is not affected by any of the governor settings.

7.4 Case C: Different Hydraulic Models

Previously the regulating machines has been modelled with the same hydraulic models, and a low-frequency oscillation connected to the surge tank has been observed. None of the hydro power plants in the real power system are alike, hence they will all have different characteristics and mass oscillations. The impact of different hydraulic models and parameters will be studied in this case.

7.4.1 Classical and IEEE

First the impact of using the IEEE model for machine G1 and the Classical model for G3 was studied. The parameter values used for the models are the same as earlier and the result is presented in Figure 7.5.

As seen in Figure 7.5 the low-frequency oscillation will have a lower amplitude, but is still poorly damped. The reason for the lower amplitude is that there is only one surge tank in this system. The mass oscillation will only occur for the hydro power plant with generator G1, but it will affect the whole system. The eigenvalues with imaginary part lower than 0.1 Hz is shown in Table 7.5.

There will only be one eigenvalue related to the mass oscillation since there is only one machine that are modelled with the IEEE model. This eigenvalue is $\lambda_{C,2}$ and as seen in Table 7.5 it is poorly damped.

7.4.2 IEEE with Different Parameters

In this part both the machines were again equipped with the IEEE model. For machine G1 the same parameter values were used as earlier, but for the hydraulic model at machine G3 the surge tank storage constant C_s was set to 100 seconds.

Table 7.5 – Eigenvalues with the IEEE and Classical model

Number	**Eigenvalue** Real part [1/s], Imaginary part [Hz]	**Damping ratio**
$\lambda_{C,1}$	$-0.384430 \pm j0.030864$	89.3%
$\lambda_{C,2}$	$-0.005275 \pm j0.010118$	8.27%
$\lambda_{C,3}$	$-0.013475 \pm j0.002325$	67.8%

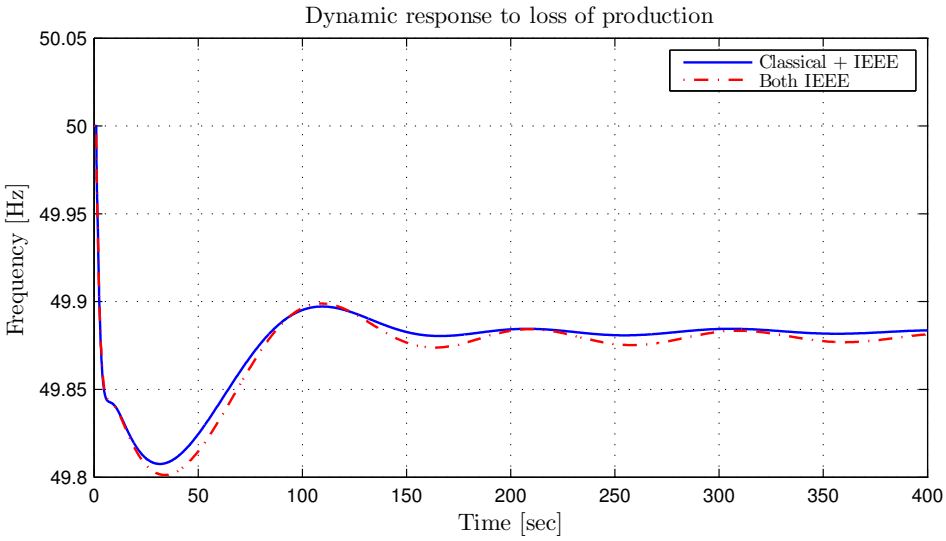

Figure 7.5 – Response with different hydraulic models on G1 (IEEE) and G3 (Classical)

In theory will the two hydro power plants now have different mass oscillation frequency. How this affect the frequency of the grid is illustrated in Figure 7.6 and the eigenvalues for the same case is presented in Table 7.6.

The eigenvalues in Table 7.6 supports the theory that the two hydro power plants now will have their own mass oscillation connected to their surge tank time constant, this is why $\lambda_{C,5}$ and $\lambda_{C,6}$ has different frequencies. $\lambda_{C,6}$ is the same eigenvalue as found in earlier studies with C_s=152.65 seconds, hence this eigenvalue represents the mass oscillation for G1. $\lambda_{C,5}$ has a higher frequency due to the lower value of C_s for the hydro power plant G3. The response is plotted as the blue curve in Figure 7.6 and it differs from the red curve that represents the case with equal

Table 7.6 – Eigenvalues with the IEEE model with different parameters for C_s

Number	**Eigenvalue** Real part [1/s], Imaginary part [Hz]	**Damping ratio**
$\lambda_{C,4}$	$-0.342930 \pm j0.030468$	87.30%
$\lambda_{C,5}$	$-0.004002 \pm j0.012532$	5.08%
$\lambda_{C,6}$	$-0.005320 \pm j0.010130$	8.33%

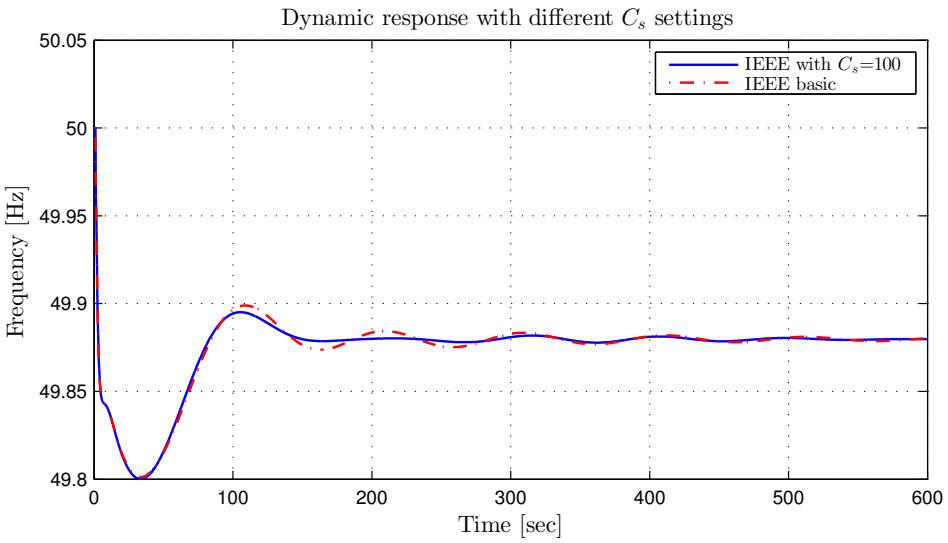

Figure 7.6 – Response with different C_s for G1 and G3

models. The response is flat from t=150-250 seconds before an oscillations starts which is almost identical to the response where equal models were used.

The relationship between the turbine head and the frequency was presented in Figure 7.3c in Case A were the response in head was plotted for different values of f_{p2}. For Case A, since the turbines were modelled equally, the mass oscillations occurred with the same frequencies. For the case with different surge tanks the mass oscillations will have different frequencies as illustrated in Figure 7.7 by the green and blue dotted line. The difference in the value for the head of G1 and G3 is caused by the difference in power output.

In Figure 7.7 the black curve is calculated as the average head and as illustrated will this give a response that looks similar to the response in frequency. The reason for the flat response between t=150-250 seconds is that the head for G1 and G3 almost equalize each other, but due to the higher value of G3 there will be a small peak.

7.4.3 Findings

The fluctuation in frequency will be a sum of the mass oscillations, which means that the response in frequency will be more "erratic". In this case this was only

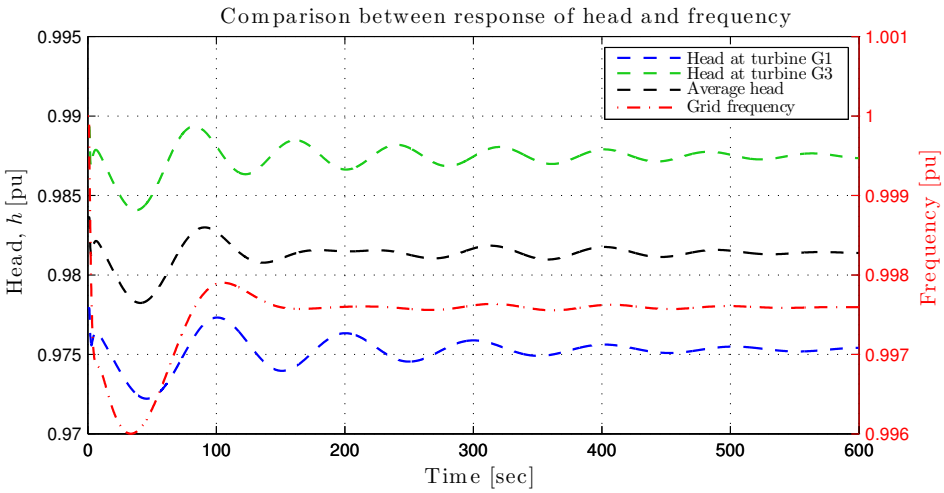

Figure 7.7 – Comparison of the response of the head for turbine G1(blue) and G3(green). The black curve is calculated as the average head at the two turbines and the red is the grid frequency

illustrated with two different mass oscillations. In the real power system there are many hydro power plants and none of them will have the same response, hence the the response in frequency will be more floating than the one indicated in Figure 7.7.

Another observation is that the variation in frequency does not affect the mass oscillation in the water conduit. The mass oscillation will continue with it's own frequency until it is damped by losses in the tunnel.

7.5 Case D: Correction for the Tunnel Water Starting Time

Towards the end of the Master's Thesis work further insight in the IEEE model was obtained. The mass oscillations that occur between the surge tank and the reservoir has a frequency given by Equation 4.18. In Case A this frequency was calculated to be 5.6 mHz, and it is this oscillation that cause the floating in the grid frequency. The oscillation in grid frequency was found to be 10.1 mHz. The reason for this difference was discovered during the last two weeks of the work on this Thesis. It is caused by a wrong value for the water starting time T_{w2}. T_{w2} is the tunnel water starting time, but for Case A, B and C the value for the penstock, T_w, has been used.

As mentioned in the introduction to the case study it has also been a mix-up for the friction factors f_{p1} and f_{p2}. f_{p1} is the penstock friction factor, but has been used as the tunnel friction factor in Case A, B and C. f_{p2} has been used for f_{p1}. The reason for this is that it has been difficult to interpret the IEEE model and the paper describing it.

7.5.1 New Simulation

A new simulation was done with both machines represented with the IEEE hydraulic model and the Classical governor. The parameters were set to be the values presented in Table A.8 in Appendix A, which means that T_{w2}=5.242, f_{p1}=0.0112 and f_{p2}=0.0372. The new eigenvalues are presented in Table 7.7.

As seen in Table 7.7 the two eigenvalues corresponding to the mass oscillations, $\lambda_{D,2}$ and $\lambda_{D,3}$, has a frequency of approximately 5,6 mHz. This corresponds to the calculated value of the mass oscillation. If the eigenvalues are compared with the

Table 7.7 – Eigenvalues with corrected values

Number	**Eigenvalue** Real part [1/s], Imaginary part [Hz]	**Damping ratio**
$\lambda_{D,1}$	$-0.343120 \pm j0.030470$	87.31%
$\lambda_{D,2}$	$-0.003969 \pm j0.005593$	11.22%
$\lambda_{D,3}$	$-0.005611 \pm j0.005563$	15.85%

eigenvalues found in Table 7.2 one can see that the damping is higher. This is due to the higher friction in the tunnel, which is now approximately three times higher than in the previous cases.

The response is plotted in Figure 7.8 and indicates that the response is similar to the response found in Case A. The frequency is measured to be 5.3 mHz and the damping 6.7%. With the changes done in Case D the only effect will be to get increased damping and a lower mass oscillation frequency. How the surge tank and friction loss affect the response will be the same.

The governor parameters will also have the same effect with the corrected values. This is illustrated for changes in T_R in Figure 7.9. The impact of higher values of T_R is a slower response and a higher amplitude for the first fluctuation. The response in Figure 7.9 is also very similar to the corresponding plot in Figure 7.4a in Case B.

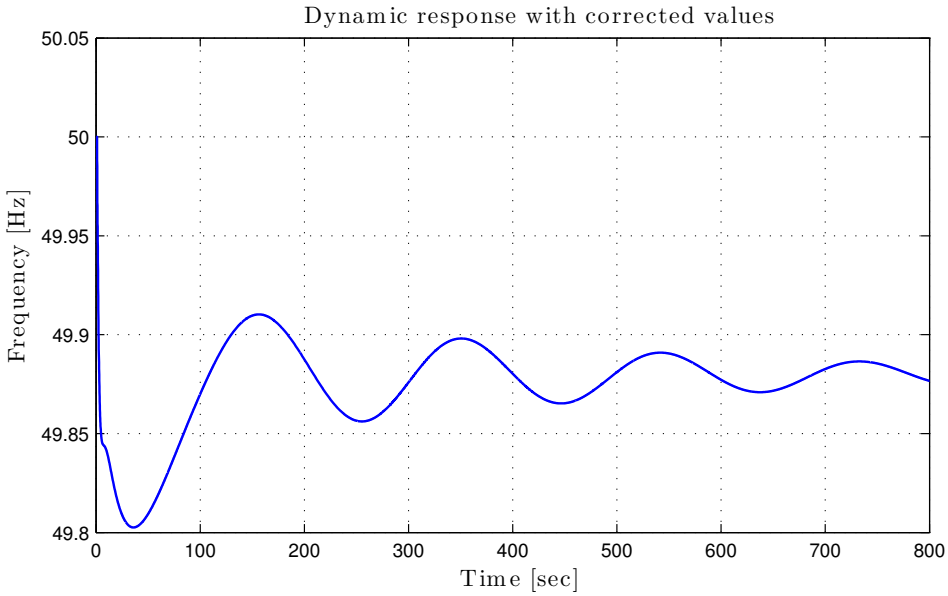

Figure 7.8 – The response with T_{w2}=5.242, f_{p1}=0.0112 and f_{p2}=0.0372

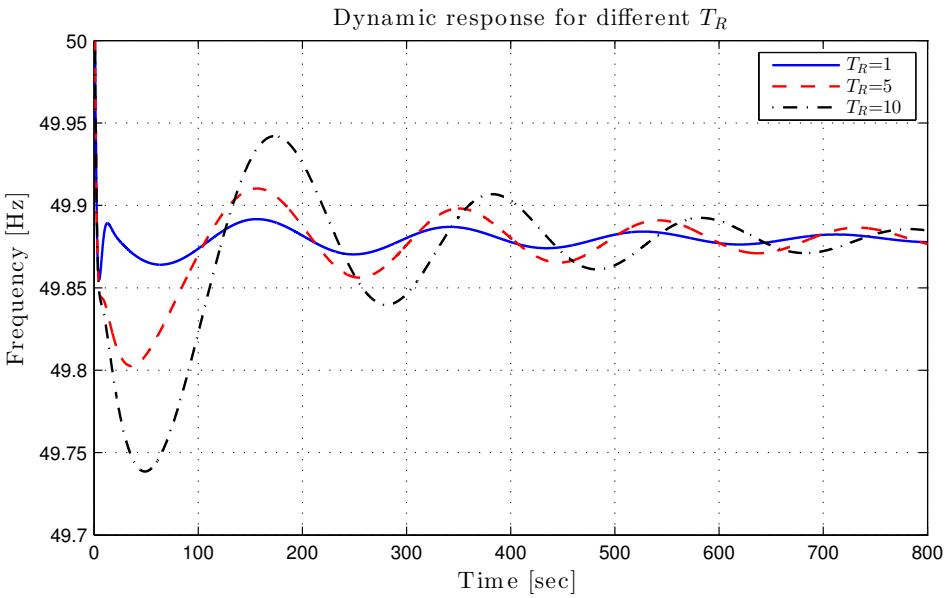

Figure 7.9 – The response with different values for T_R

7.5.2 Findings

It has been shown that with the use of a more correct value for T_{w2} the frequency of the simulated oscillation will be equal to the calculated frequency for the mass oscillation that occur between the surge tank and the reservoir. Other than this the response will be similar to the response with other values for T_{w2} and the governor parameters will have the same impact.

It is worth mentioning that the parameters used in this case study are just one example for one kind of hydro power plant. With different tunnels, penstocks and surge tanks follow different mass oscillation frequencies. In this case the frequency was found to be 5.6 mHz, but for other hydro power plants this frequency can be higher or lower.

Chapter 8

Limitations and Discussion

This chapter will briefly point out the limiting factors in this Master's Thesis and discuss how they affect the results.

8.1 Simulation Software

SIMPOW® is as described in Chapter 3 a comprehensive tool for performing different kinds of power system analyses, both stationary and dynamic. SIMPOW® has limitations regarding available models for hydro power stations. The implemented hydraulic models lack the water hammer effect and the mass oscillation caused by the surge tank.

Another limitation in this Thesis is the lack of sensitivity analysis, which might have been an appropriate contribution as part of the linear analysis. Via the sensitivity analysis one can find the factor that contribute most to different modes, and how the modes change with respect to different parameter values. The linear analysis tool in SIMPOW® failed, however, in this context. This is due to non-linear or badly implemented models and limitations in the way SIMPOW® perform the calculations.

8.2 Hydraulic System Modelling

In this Thesis the main goal has been to study the impact of the governor on low-frequency oscillations by using already implemented hydraulic models. The implemented models in SIMPOW® does not consider the effects of the water

hammer and the surge tank, and much time has been spent on understanding and verifying the more detailed models developed by previous Master students.

It has been difficult to find parameter values for the hydraulic models. In this Thesis the parameter values used were found in a IEEE paper, but there still were difficulties in understanding and calculating the values to be used in the model [12]. Wrong value was used for the water starting time for the tunnel during the first three cases, hence there were problems in getting the frequency of the calculated and simulated oscillations to correspond. The friction factors were also mixed which means that the oscillations should be better damped for the first three cases.

The results of the first three cases are nevertheless not insignificant. With use of the wrong value for T_{w2} the oscillations will only occur with different frequencies, and in Case D it was shown that the same kind of response in frequency is obtained with a more correct value of T_{w2} and correct friction coefficients for the tunnel and penstock. The governor reset time was also found to have the same impact for Case D, which indicates that the results from Case B is valid.

8.3 Power System Model

The reduced system model is a three-machine equivalent of the interconnected Norwegian and Swedish power system. To make one machine act dynamically like all the machines in Norway is not possible and the model will be a simplification no matter how this is tuned. In the reduced system model values for one hydro power plant is used and scaled to represent a large power plant.

The equivalent used in this Thesis is nevertheless a model that can indicate how the Norwegian and Swedish power system act dynamically under a large disturbance. It is for instance possible to see how the generators in Norway will swing in relation to the generators in Sweden. The frequency of the oscillations found in this Thesis are so low that all the generators in the power system swing together.

One significant limitation with this model is given by the fact that it is only possible to simulate the effect of two different hydraulic systems. It was shown that the oscillation in frequency will be a sum of the mass oscillations, hence the power system frequency will be more "erratic". In the Norwegian and Swedish power systems there are a lot of different hydro power plants, so its obvious that the frequency will be more floating as indicated in Figure 1.1 in Chapter 1.

Chapter 9

Conclusion

This Master's Thesis has studied the impact of detailed hydraulic models on the response of the grid frequency in an equivalent of the Norwegian and Swedish power system. It has been shown that there is a significant difference between the standard models implemented in power system analysis tools and the more detailed models presented in literature. The detailed model, here represented by the IEEE model, includes the effect of the surge tank which was found to give a mass oscillation that affect the pressure at the turbine. The pressure oscillation can cause a slow floating in the grid frequency.

For the reduced system model it has been illustrated that the fluctuation in the frequency of the grid will be a sum of the different mass oscillations. This implicate that the floating in grid frequency will be "erratic" since it consist of several sinusoidal oscillations with different frequencies. This is also the case for the measured frequency in the Nordic power system.

The turbine governor parameters has little influence on the low-frequency oscillation. It has been illustrated that with a higher time constant for the reset time and a higher temporary droop, which implicate lower gain, the response will be slower and the first fluctuation will have higher amplitude. The damping of the mass oscillation remains poor.

Chapter 10

Further Work

This chapter will present suggestions to scope for further work.

10.1 Governor Modelling

The impact of dead bands has not been studied in this Thesis. For the Classical governor a dead band has been implemented, but in real systems its difficult to find data that identify their magnitude. How dead bands will affect the response is of great interest and should be studied further.

10.2 Hydraulic System Modelling

10.2.1 The Models

For further work a deeper research into hydraulic modelling is suggested. The implementation of models into SIMPOW® is time consuming and difficult for those who don't have the necessary skills in DSL-programming. The models need to be accurate and functional for all kinds of cases. This means that the models must be able to undergo situations where special requirements to mathematical modelling are necessary, for example initial conditions for derivatives and how to cope with non-linearities.

The IEEE model includes a surge tank and head losses related to the surge tank, tunnel and penstock. In many hydro power plants the water conduit is more comprehensive and can have several tunnels, penstocks and surge tanks,

both upstream and downstream of the turbine. This can in theory cause several mass oscillations and a more complex response. It is very extensive work if all the different hydro power plants should be modelled in detail, but it would be interesting to see how several surge tanks will affect the response for one hydro power plant.

10.2.2 Parameters

As discussed in Chapter 8 there were difficulties in the interpretation of the different parameter values to use with the IEEE model. For the reduced system model used in this Thesis parameter values reflecting one specific hydro power plant were used. To use values for a typical Norwegian and Swedish power plant would be interesting.

Since the parameters were converted to per unit the model can simulate a 15 GW hydro power plant. This will in fact not be an equivalent of the hydro power plants in Norway and Sweden, but just a way of scaling one hydro power plant. To make a realistic equivalent of the hydro power plants in Norway and Sweden an average of the real values should be used. This is time consuming and difficult, but it is a measure to make the reduced system model more realistic.

10.3 Sensitivity Analysis

Sensitivity analysis has not been carried out in this Thesis. A sensitivity analysis would be a good method to find out how the mode associated with the mass oscillation is affected by different parameters. Badly implemented hydraulic models can be one of the reasons for the linear analysis tool of SIMPOW® to fail. The DSL-file for the IEEE model should therefore be studied further in order to make a model that can cope with sensitivity analysis. Another suggestion is to find out if it's possible to make a linear model that includes the effect of the mass oscillation.

10.4 Power System Model

The reduced system model is a small equivalent of the Norwegian and Swedish power system and since it's only modelled with two machines supplying primary regulation it is limitations to how the effect of different hydraulic system

characteristics can be simulated. The next step would be to make a more extensive equivalent of the Norwegian and Swedish grid and also include the rest of the Nordic power system. Certain models do already exist and are developed by Statnett for the simulation tool PSS®E. There are methods to convert these models to files that can be used in SIMPOW®.

References

[1] Jonas Person, Anders Frisk, and Lovisa Stenberg. *Identification of Frequency Response in the Nordel System.* Vattenfall Research and Development AB, 2011.

[2] Morten Hemmingsson. *Report 60-90s oscillations in the Nordic power system 2005-2011.* Gothia Power, 2012.

[3] Nordel's Planning Committee. *Nordic Grid Code 2007.* Nordel, 2007. Can be found at: `https://www.entsoe.eu/index.php?id=62`.

[4] P. Kundur, J. Paserba, V. Ajjarapu, G. Andersson, A. Bose, C. Canizares, N. Hatziargyriou, D. Hill, A. Stankovic, C. Taylor, T. Van Cutsem, and V. Vittal. Definition and classification of power system stability ieee/cigre joint task force on stability terms and definitions. *Power Systems, IEEE Transactions on*, 19(3):1387 – 1401, aug. 2004.

[5] Yiping Dai, Pan Zhao, and Shuping Chang. Primary frequency control characteristic of a grid. In *Industrial Electronics and Applications, 2008. ICIEA 2008. 3rd IEEE Conference on*, pages 1493 –1497, june 2008.

[6] G. Rogers. Demystifying power system oscillations. *Computer Applications in Power, IEEE*, 9(3):30 –35, jul 1996.

[7] Jan Machowski, Janusz W. Bialek, and James R. Bumby. *Power System Dynamics - Stability and Control.* John Wiley and Sons, Ltd., 2nd edition, 2008.

[8] Prabha Kundur. *Power System Stability and Control.* Teta McGraw-Hill, 2006.

[9] Jens G. Balchen, Trond Andresen, and Bjarne A. Foss. *Reguleringsteknikk.* Institutt for teknisk kybernetikk, NTNU, 5th edition, 2004.

[10] Øyvind Rue. *SIMPOW® Power system simulation software User Manual 11.0.* STRI AB, Sweden, 2010.

[11] Nand Kishor, S.P. Singh, and A.S. Raghuvanshi. Dynamic simulations of hydro turbine and its state estimation based lq control. *Energy Conversion and Management*, 47:3119 – 3137, 2006.

[12] Hydraulic turbine and turbine control models for system dynamic studies. *Power Systems, IEEE Transactions on*, 7(1):167 –179, feb 1992.

[13] Hermod Brekke. *Pumper og Turbiner*. Vannkraftlaboratoriet, NTH, 1995.

[14] Hermod Brekke. *A stability study on hydro power plant governing including the influence from a quasi nonlinear damping of oscillatory flow and from the turbine characteristics, VOLUME I*. NTH, 1984.

[15] Ola Høydal Helle. Electric hydraulic interaction. Master's thesis, NTNU, 2011.

[16] Sa'ad Mansoor. Behaviour amd operation of pumped storage hydro plants. Master's thesis, University of Wales. Bangor, 2000.

[17] Torbjørn K. Nielsen. *Dynamisk Dimensjonering av Vannkraftverk*. SINTEF Strømningsmaskiner, 1990.

[18] Luz Alexandra Lucero Tenorio. Hydro turbine and governor modelling - electric-hydraulic interaction. Master's thesis, NTNU, 2010.

[19] Liang Fu, Jiandong Yang, Haiyan Bao, and Jinping Li. Effect of turbine characteristic on the response of hydroturbine governing system with surge tank. In *Power and Energy Engineering Conference, 2009. APPEEC 2009. Asia-Pacific*, pages 1 –6, march 2009.

[20] D.G. Ramey and J.W. Skooglund. Detailed hydrogovernor representation for system stability studies. *Power Apparatus and Systems, IEEE Transactions on*, PAS-89(1):106 –112, jan. 1970.

[21] Nordel Statistics Group. *Annual Report 2008*. Nordel, 2009. Can be found at `https://www.entsoe.eu/index.php?id=65`.

[22] Jonas Persson. *Kundur´s Two-Area System*. STRI AB, 1996. Can be found at `http://simpow.com/Kundurs-Two-Area-System.pdf`.

[23] Liang Fu, Jiandong Yang, Haiyan Bao, and Jinping Li. Effect of turbine characteristic on the response of hydroturbine governing system with surge tank. In *Power and Energy Engineering Conference, 2009. APPEEC 2009. Asia-Pacific*, pages 1 –6, march 2009.

Appendix A

Parameters

A.1 System Parameters

Table A.1 – Line parameters

Parameter		Value
Line resistance	R_{line}	0.0024 Ω
Line reactance	X_{line}	0.0570 Ω
Line susceptance	B_{line}	$81.74 \cdot 10^{-6}$ 1/Ω

Table A.2 – Line lengths

Bus	Length
Bus 6 - Bus 7, Bus 8 - Bus 12 and Bus 9 - Bus 10	10 km
Bus 7 - Bus 9	150 km
Bus 7 - Bus 8 and Bus 8 - Bus 9	100 km

Table A.3 – Transformer parameters

Parameter		Value
Rated power	S_n	20 GVA
Primary voltage	U_p	20 kV
Secondary voltage	U_s	420 kV
Short circuit reactance	X_{sc}	0.15 pu

A.2 Synchronous Machines

Table A.4 – Parameters for the synchronous machines

Parameter		Value
Inertia	H	6.5 s
Rated power	S_n	22 GVA
Stator resistance	R_a	0.0025 pu
Stator leakage reactance	X_l	0.2 pu
Direct-axis synchronous reactance	X_d	1.8 pu
Direct-axis transient reactance	X'_d	0.3 pu
Direct-axis subtransient reactance	X''_d	0.25 pu
Quadrature-axis synchronous reactance	X_q	1.7 pu
Quadrature-axis transient reactance	X'_q	0.55 pu
Quadrature-axis subtransient reactance	X''_q	0.25 pu
D-axis open-ciruit transient time constant	T'_{d0}	8.0 s
D-axis open-ciruit subtransient time constant	T''_{d0}	0.03 s
Q-axis open-ciruit transient time constant	T'_{q0}	0.4 s
Q-axis open-ciruit subtransient time constant	T''_{q0}	0.05 s

A.3 Exciter and PSS

Table A.5 – Parameters for the excitation system

Parameter	Value
KA	200
TR	0.01

Table A.6 – Parameters for the power system stabilizer

Parameter	Value
$KSTAB$	20
TW	10
$T1$	0.05
$T2$	0.02
$T3$	3.0
$T4$	5.4

A.4 Hydro Power Plant

Table A.7 – Hydro Power Plant Data [12]

Parameter		Value
Rated generator MVA		100 MVA
Rated turbine power		90.94 MW
Rated turbine flow	q_{base}	71.43 m^3/s
Rated turbine head	h_{base}	138.9 m
No-Load flow	q_{nl}	4.3 m^3/s
Reservoir head		307.0 m
Tail head		166.4 m
Penstock length		465 m
Penstock cross section		15.2 m^2
Penstock wave velocity		1100 m/s
Penstock head loss coefficient	f_{p1}	0.0003042 $m/(m^3/s)^2$
Tunnel length		3850 m
Tunnel cross section		38.5 m^2
Tunnel wave velocity		1200 m/s
Tunnel head loss coefficient	f_{p2}	0.0010112 $m/(m^3/s)^2$
Surge tank cross section		78.5 m^2
Surge tank head loss coefficient	f_0	0.0040751 $m/(m^3/s)^2$

A.5 Hydraulic Models

The values in the following tables are derived from Table A.7 and the equations in Chapter 4. The calculation of the parameters can be found in Appendix E.

Table A.8 – Parameters for the IEEE model

Parameter		Value
Storage constant surge tank	C_s	152.65
Surge impedance of penstock	Z_0	3.794
Water starting time penstock	T_w	1.604
Water starting time tunnel[1]	T_{w2}	5.242
Friction factor surge tank	f_0	0.1498
Friction factor penstock[2]	f_{p1}	0.0112
Friction factor tunnel[2]	f_{p2}	0.0372
Proportional factor	A_T	1.0
Penstock elastic time constant	T_e	0.4227
Damping	D	0.5
No-load flow	q_{nl}	0.0602

[1]This value was only used in Case D.
In the other cases T_{w2} was set to the value of T_w.
[2]These values were mixed up during Case A, B and C

Table A.9 – Parameters for the Classical model

Parameter		Value
Water starting time	T_w	1.604
Proportional factor	A_T	1.0
Damping	D	0.5
No-load flow	q_{nl}	0.0602

A.6 Governors

Table A.10 – Typical parameters for the Classical governor [8]

Parameter		Value
Permanent droop	R_P	0.06
Temporary droop	R_T	0.40
Pilot valve time constant	T_P	0.05
Reset time	T_R	5.00
Main servo time constant	T_G	0.20
Servo gain	K_S	5.00

Table A.11 – Parameters for the PID model

Parameter		Value
Permanent droop	R_P	0.06
Pilot valve time constant	T_P	0.05
Main servo time constant	T_G	0.2
Proportional gain	K_P	3.4
Integral gain	K_I	1.0
Derivative gain	K_D	2.2

The following values are found by using equations presented in Chapter 5.6.

Table A.12 – Recommended values

Parameter		Value
Temporary droop	R_T	0.2726
Reset time	T_R	7.5356
Proportional gain	K_P	6.4838
Integral gain	K_I	1.2127
Derivative gain	K_D	0.4331

Appendix B

Optpow File

```
This is the Optpow file for the reduced system model which
is a 3 bus equivalent of the Swedish and Norwegian grid.
This model is based upon the Kundur Two–Area model.
**  reducedmodel.optpow  **
GENERAL
 SN=1000
END

CONTROL DATA
NPRD=100
END

NODES
  BUS1    UB=20    AREA=1
  BUS3    UB=20    AREA=2
  BUS6    UB=420   AREA=1
  BUS7    UB=420   AREA=1
  BUS8    UB=420   AREA=3
  BUS9    UB=420   AREA=2
  BUS10   UB=420   AREA=2
  BUS12   UB=420   AREA=3
  BUS14   UB=20    AREA=3
END

TRANSFORMERS
```

```
 BUS1   BUS6   SN=20000 UN1=20 UN2=420 ER12=0 EX12=0.15
 BUS14   BUS12 SN=20000 UN1=20 UN2=420 ER12=0 EX12=0.15
 BUS3   BUS10 SN=20000 UN1=20 UN2=420 ER12=0 EX12=0.15
END

LINES
 BUS6   BUS7    TYPE=2 R=0.0024 X=0.057
                     B=0.00000081744 L=10
 BUS12   BUS8   TYPE=2 R=0.0024 X=0.057
                     B=0.00000081744 L=10
 BUS9   BUS10   TYPE=2 R=0.0024 X=0.057
                     B=0.00000081744 L=10
 BUS7   BUS9    TYPE=2 R=0.0024 X=0.057
                     B=0.00000081744 L=150
 BUS7   BUS8    TYPE=2 R=0.0024 X=0.057
                     B=0.00000081744 L=100
 BUS8   BUS9    TYPE=2 R=0.0024 X=0.057
                     B=0.00000081744 L=100
END

LOADS
 BUS7   P=14100    Q=1000   MP=0   MQ=0 NO=1
 BUS7   P=-1600    Q=0 MP=0 MQ=0 NO=2
 BUS9   P=12300   Q=1000   MP=0   MQ=0
 BUS8   P=10500   Q=1000   MP=0   MQ=0
END

POWER CONTROL
 BUS1    TYPE=NODE   RTYP=UP   U=20.6   P=15000     NAME=G1
 BUS3    TYPE=NODE   RTYP=SW   U=20.6   FI=-6.8   NAME=G3
 BUS14   TYPE=NODE   RTYP=UP   U=20.6   P=10000     NAME=G5
END

END
```

Appendix C

One-Line Diagram

The one line diagram for the reduced system model is presented on the next page.

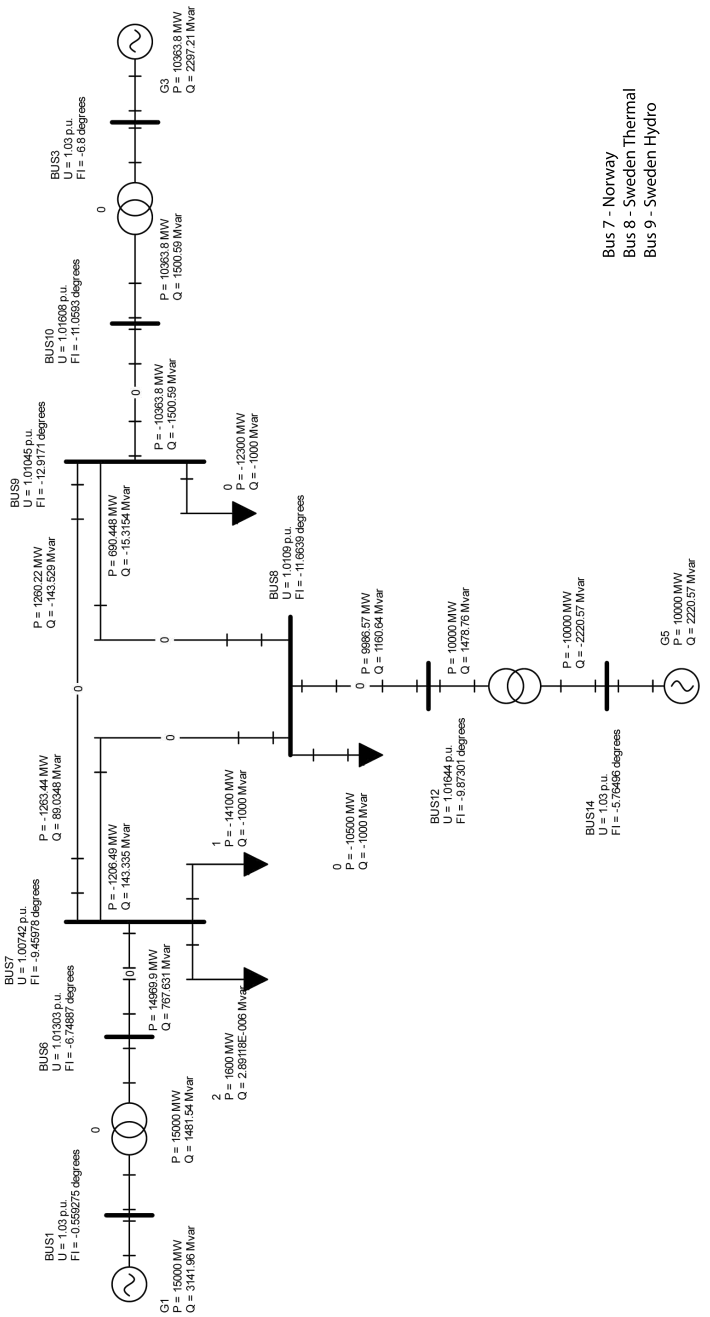

Figure C.1 – The reduced system model

Appendix D

Dynpow File

Comments to the Dynpow File

For the IEEE model some of the parameters have different names in the implemented model and in the block diagram presented in Chapter 4. The block diagram parameters and the corresponding Dynpow parameters are listed in Table D.1.

Table D.1 – Parameters used in Dynpow

IEEE model	**Dynpow**
f_{p1}	FF_P
f_{p2}	FF_T
f_0	FF_S
T_e	TE2
T_{w2}	TW_T
D	KD

```
The Dynpow file used for the case study.
** case.dynpow **
CONTROL DATA
  TEND=600
  TETL=180
END
GENERAL
  FN=50
END
SYNCHRONOUS MACHINE
```

```
G1    BUS1    TYPE=1   XD=1.8 XQ=1.7 XA=0.2 XDP=0.3
                       XQP=0.55 XDB=0.25 XQB=0.25
                       RA=0.0025 TD0P=8.0 TQ0P=0.4
                       TD0B=0.03 TQ0B=0.05 TAB=1
                       TURB=11 H=6.5 SN=22000
                       UN=20 D=0 VREG=2
G3    BUS3    TYPE=1   XD=1.8 XQ=1.7 XA=0.2 XDP=0.3
                       XQP=0.55 XDB=0.25 XQB=0.25
                       RA=0.0025 TD0P=8.0 TQ0P=0.4
                       TD0B=0.03 TQ0B=0.05 TAB=1
                       TURB=11 H=6.25 SN=22000
                       UN=20 D=0 VREG=2
G5    BUS14   TYPE=1 XD=1.8 XQ=1.7 XA=0.2 XDP=0.3
                       XQP=0.55 XDB=0.25 XQB=0.25
                       RA=0.0025 TD0P=8.0 TQ0P=0.4
                       TD0B=0.03 TQ0B=0.05 TAB=1
                       TURB=0 H=6.175 SN=22000
                       UN=20 D=0 VREG=2
END

REGULATORS
2       TYPE=DSL/EXC_HTG/       KA=200 TR=0.01
                       SWS=4
4       TYPE=DSL/STABILISER/ KSTAB=20 TW=10
                       T1=0.05 T2=0.02 T3=3 T4=5.4
END

DSL-TYPE
 STABILISER(W,T4,T3,T2,T1,TW,KSTAB,VS,VS0)
 EXC_HTG(VC,TR,KA,VS/0/,UF,UF0)
 KundurGOV(RP,RMAXO,RMAXC,KS,
         TK,TR1,TR2,RT,
         TG,GMAX,GMIN,TP,
         W,Y,Y0)
 PIDGOV(TD,KD,KI,KP,
         RP,RMAXO,RMAXC,KS,
```

```
        TK,TG,GMAX,GMIN,
        TP,W,Y,Y0)
 KundurDB(DB,RP,RMAXO,RMAXC,
        KS,TK,TR1,TR2,
        RT,TG,GMAX,GMIN,
        TP,W,Y,Y0)
 CLASSICAL(TW/0/,Y,W,DEMPING/0/,AT/0/,QNL/0/,TM,TM0)
 IEEE(FF_P/0/,W,Z0/0/,TE2/0/,FF_T/0/,CS/0/,FF_S/0/,
 TW_T/0/, KD/0/,AT/0/,QNL/0/,Y,TM,TM0)
END

TURBINES
!!! Classical and IEEE model with parameters
!!! from IEEE paper
 11  TYPE=DSL/CLASSICAL/  GOV=20 TW=1.604 AT=1.0
                          QNL=0.0602 DEMPING=0.5
 12  TYPE=DSL/IEEE/ GOV=20 FF_P=0.0112 Z0=3.794
                          TE2=0.4227 FF_T=0.0372 CS=152.65
                          FF_S=0.1498 TW_T=5.242 KD=0.5
                          AT=1.0 QNL=0.0602

!! IEEE model with other parameters
 13  TYPE=DSL/IEEE/ GOV=21 FF_P=0.03 Z0=2.8
                          TE2=0.5 FF_T=0.0015 CS=50
                          FF_S=0.10 TW_T=1.4 KD=0.5
                          AT=1.0 QNL=0.0602

!!! KundurGOV with basic parameters
 20 TYPE = DSL/KundurGOV/ RP=0.06 RMAXO=0.1 RMAXC=-0.1
                          KS=5 TK=0 TR1=5 TR2=5
                          RT=0.4 TG=0.2 GMAX=1.0 GMIN=0
                          TP=0.05

!!! PIDGOV and KundurGOV with recommended parameters
 30 TYPE = DSL/KundurGOV/ RP=0.06 RMAXO=0.1 RMAXC=-0.1
                          KS=5 TK=0 TR1=7.5356 TR2=7.5356
```

```
                                RT=0.2726 TG=0.2 GMAX=1.0
                                GMIN=0 TP=0.05
 31 TYPE = DSL/PIDGOV/          TD=0.1 KD=0.4331 KI=1.2127
                                KP=6.4838 RP=0.06 RMAXO=0.1
                                RMAXC=-0.1 KS=1.0 TK=0 TG= 0.2
                                GMAX=1.0 GMIN=0 TP=0.02

!!! KundurGOV with deadband (DB)
 22 TYPE = DSL/KundurDB/        DB=0 RP=0.06
                                RMAXO=0.1 RMAXC=-0.1
                                KS=5.0 TK=0 TR1=5 TR2=5
END

LOADS
 BUS7 NO=1 MP=1 MQ=2
 BUS7 NO=2 MP=1 MQ=2
 BUS8 MP=1 MQ=2
 BUS9 MP=1 MQ=2
END

!!!! Below follows saturation characteristic
!!!! for the synchronous machines.
!!!! See section 3.1.2 in the document
!!!! "Kundur's Two-Area System".
TABLES
 1 TYPE=1 F 0.000 0.00 0.700 0.70
            0.800 0.80 0.830 0.83
            0.860 0.86 0.962 0.94
            0.974 0.95 1.039 1.00
            1.113 1.05 1.202 1.10
            1.315 1.15 1.467 1.20
            1.682 1.25 1.998 1.30
            2.478 1.35
 2 TYPE=0 F 0.000 1.00
END
```

```
RUN INSTRUCTION
!!! Disconnects the power injection at Bus 7
 AT 1.050 INST DISCONNECT LOAD BUS7 NO=2
END

END
```

Appendix E

Calculation of Parameters

Here follows calculation of the different parameters used in the IEEE model. The equations can be found in Chapter 4 and the values are given in Table A.7.

T_w is found with Equation 4.9 and is the water starting time for the penstock:

$$T_w = \frac{465\,\text{m} \cdot 71.43\,\text{m}^3/\text{s}}{15.2\,\text{m}^2 \cdot 138.9\,\text{m} \cdot 9.81\,\text{m/s}^2} = 1.604\,\text{s} \tag{E.1}$$

The wave travel time for the penstock, T_e, is found with Equation 4.12:

$$T_e = \frac{465\,\text{m}}{1100\,\text{m/s}} = 0.423\,\text{s} \tag{E.2}$$

Z_0 is found with Equation 4.11 and is the surge impedance for the penstock:

$$Z_0 = \frac{1.604\,\text{s}}{0.423\,\text{s}} = 3.794 \tag{E.3}$$

The surge tank storage constant, C_s, is found with Equation 4.17:

$$C_s = \frac{78.5\,\text{m}^2 \cdot 138.9\,\text{m}}{71.43\,\text{m}^3/\text{s}} = 152.65\,\text{s} \tag{E.4}$$

q_{nl} was found by using the base value of the flow:

$$q_{nl} = \frac{4.3\,\text{m}^3/\text{s}}{71.43\,\text{m}^3/\text{s}} = 0.0602\,\text{pu} \tag{E.5}$$

To find the per unit values of the frictional factors the base value for the frictional

loss was found with Equation 4.20 with the base values of the head and flow.

$$f_{base} = \frac{138.9\ \text{m}}{71.43^2\ (\text{m}^3/\text{s})^2} = 0.02722\ \text{m}/(\text{m}^3/\text{s})^2 \tag{E.6}$$

The different frictional factors were then calculated with this base value to get per unit values:

$$f_0 = \frac{0.0040751}{0.02722} = 0.1498\ \text{pu} \tag{E.7}$$

$$f_{p1} = \frac{0.0003042}{0.02722} = 0.0112\ \text{pu} \tag{E.8}$$

$$f_{p2} = \frac{0.0010112}{0.02722} = 0.0372\ \text{pu} \tag{E.9}$$

The water starting time for the tunnel, T_{w2}, was found with the same equation as for T_w, but with values for the tunnel.

$$T_{w2} = \frac{3850\ \text{m} \cdot 71.43\ \text{m}^3/\text{s}}{38.5\ \text{m}^2 \cdot 138.9\ \text{m} \cdot 9.81\ \text{m/s}^2} = 5.242\ \text{s} \tag{E.10}$$

The proportional factor A_T has been set to 1 since it was difficult to find the correct values for q_r and h_r. Since its only a proportional factor it will only have influence on the steady state values and will not cause any significant difference for the dynamic response.